

Learning the Interference Graph of a Wireless Network

Jing Yang, *Member, IEEE*, Stark C. Draper, *Senior Member, IEEE*, Robert Nowak, *Fellow, IEEE*

Abstract—A key challenge in wireless networking is the management of interference between transmissions. Identifying which transmitters interfere with each other is a crucial first step. In this paper we cast the task of estimating the a wireless interference environment as a graph learning problem. Nodes represent transmitters and edges represent the presence of interference between pairs of transmitters. We passively observe network traffic transmission patterns and collect information on transmission successes and failures. We establish bounds on the number of observations (each a snapshot of a network traffic pattern) required to identify the interference graph reliably with high probability.

Our main results are scaling laws that tell us how the number of observations must grow in terms of the total number of nodes n in the network and the maximum number of interfering transmitters d per node (maximum node degree). The effects of hidden terminal interference (i.e., interference not detectable via carrier sensing) on the observation requirements are also quantified. We show that to identify the graph it is necessary and sufficient that the observation period grows like $d^2 \log n$, and we propose a practical algorithm that reliably identifies the graph from this length of observation. The observation requirements scale quite mildly with network size, and networks with sparse interference (small d) can be identified more rapidly. Computational experiments based on a realistic simulations of the traffic and protocol lend additional support to these conclusions.

Index Terms—Interference graph learning, CSMA/CA protocol, minimax lower bounds, 5G cellular systems, heterogeneous networks, HetNets

I. INTRODUCTION

Due to the broadcast nature of wireless communications, simultaneous transmissions in the same frequency band and time slot may interfere with each other, thereby limiting system throughput. Interference estimation is thus an essential part of wireless network operation. Knowledge of interference among nodes is an important input in many wireless network configuration tasks, such as channel assignment, transmit power control, and scheduling.

This work was supported, in part, by the Air Force Office of Scientific Research under grant FA9550-09-1-0140, by the National Science Foundation under grants CCF-0963834, ECCS-1405403, ECCS-1650299, and by the National Sciences and Engineering Research Council of Canada through a Discovery Grant. This material was presented, in part, at the *IEEE Int. Symp. Inf. Theory*, July 2012 [1].

J. Yang is with the School of Electrical Engineering and Computer Science, The Pennsylvania State University, University Park, PA, 16802, USA. Email: yangjing@psu.edu.

S. C. Draper is with the Department of Electrical and Computer Engineering, University of Toronto, Canada. Email: stark.draper@utoronto.ca.

R. Nowak is with the Department of Electrical and Computer Engineering, University of Wisconsin-Madison, WI, 53706, USA. Email: nowak@ece.wisc.edu

A number of recent efforts have made significant progress towards the goal of real-time identification of the network interference environment. Some of the recent approaches (e.g., Interference maps [2] and Micro-probing [3]) inject traffic into the network to infer occurrences of interference. While such approaches can be quite accurate in determining interference, the overhead of making such active measurements in a large network limits their practicality. In particular, the periodic use of active probing methods to identify interference can place a significant burden on the network when network conditions change over time. Time variations can be caused by changes in the physical environment, e.g., by an office door being left open, or by mobility among the clients, or the dynamic power configuration in heterogeneous networks [4].

The desire to avoid the overhead of active probing motivates the development of passive techniques such as the “Passive Interference Estimation” (PIE) algorithm [5], [6]. Inspired by two passive WLAN (wireless local area network) monitoring approaches (Jigsaw [7], [8] and WIT [9]) PIE infers interference structure from passive observation of the pattern of successful, and unsuccessful, transmissions. Experimental studies in small testbeds [6] show that PIE is quite promising, but very little is understood about how the method scales up to large complex networks. Understanding such scaling is the focus of this paper.

We formulate passive interference estimation as a statistical learning problem. Given an arbitrary WLAN that consists of n access points (APs) and a variable number of mobile clients, our goal is to recover the “interference” or “conflict” graph among these APs with as few measurements as possible. This graph encodes the interference relations between APs and other APs’ clients. We study two versions of the problem. In the first version we study “direct” interference between APs where edges in the graph indicate that a pair of APs are within each other’s carrier sensing range. Letting d be the maximum number of interfering APs per AP, we show that to identify the conflict graph one must collect a number of measurements proportional to $d^2 \log n$. This is quite mild dependence on the network size n and indicates that interference graph inference is scalable to large networks and that sparser patterns of interference are easier to identify than denser patterns. In the second version we quantify the effect of “hidden” terminal interference. This type of interference occurs when one AP interferes with another AP’s clients, but the transmission of the interfering AP is not detectable by the other AP. In this case feedback on transmission successes and failures is required to estimate the graph. For both versions of the problem we present easy-to-implement graph estimation algorithms.

The algorithms are adaptive to d , in the sense that they do not require a priori knowledge of d . We also develop lower bounds that demonstrate that the time-complexity attained by the algorithms cannot be improved upon by any other scheme. This provides insight into the time scale over which network interference patterns can be identified and tracked in dynamically changing networks.

The inference problem studied in this paper is somewhat reminiscent of network tomography, in which one attempts to identify network parameters based on network topology-dependent measurements [10]. In [11], [12], knowledge of pairwise metric values, such as end-to-end loss, are used to identify the network topology. In [13] a network tomography approach based on network coding is discussed. The idea is to exploit the topology-dependent correlation introduced by network coding in the content of received packets to reverse-engineer the topology. For the interference graph inference problem studied in this paper, the topology information is encoded in the transmission patterns and feedback information. We use pairwise relationships of an AP's transmission status to recover the direct inference graph, and use the feedback information together with the transmission patterns to recover the hidden inference graph.

The problem of inferring the hidden interference graph studied in this paper is related to group testing problems. Group testing is a process to identify a small set of defective items from a large population through a sequence of tests. Each test is conducted on a subset of all items, where a positive outcome indicates that at least one defective item is contained in the subset. One major research direction in group testing is the design of the test matrix, and the number of tests required to effect reliable detection. In [14], the group testing problem is formulated as a channel coding/decoding problem. The test matrix is formed randomly, and the total number of tests required to identify the defective set is characterized from an information theoretic perspective. In [15] group testing on graphs is investigated. Each test must conform to the constraints imposed by the graph. A distributed group testing algorithm which detects the set of defective sensors from binary messages exchanged by the sensors is studied in [16]. The inference of a hidden inference graph studied in this paper is similar to a group testing problem in the sense that, for each AP, its hidden interferers form the set of “distinguished” APs from the whole set of APs. If AP i transmits at time t , the subset of APs that are transmitting simultaneously at time t form the test pool, and the feedback information is the test outcome. If the feedback information indicates that the transmission of AP i fails, it implies that at least one hidden interferer is within the test pool; otherwise, no hidden interferer is included in the pool. Identifying the hidden interference graph is equivalent to recover the set of “distinguished” APs for each AP. However, our problem is different from the variants of group testing problems studied to date in the following aspects. In our setting, each test corresponds to a transmission pattern in the network, which is subject to constraints imposed by the direct interference graph, and depends on the traffic statuses of all APs. Therefore, we do not get to design the test matrix in the passive interference

estimation setting. This is in contrast to other group testing problems wherein the design of test matrices can be controlled. Moreover, the complicated transmission mechanism of the APs imposes a heavily constrained structure on the design matrix, which makes existing detection methods and analyses inapplicable. In addition, to recover of the hidden interference graph we are required to perform a number of overlapped group tests for all APs in parallel. This results in quite different scaling laws of the number of tests required.

While we note that the motivating work for this paper comes from research into WLANs, we anticipate that these ideas will also find application in larger-scale cellular-type networks. In particular, consider the heterogeneous networks (HetNets) that are part of the fourth-generation Long Term Evolution (LTE) Advanced networks. In HetNets, small “femto” cells interfere with large “macro” cells. Due to the overhead required, it is preferable to discover the interference environment using passive methods, rather than active probing methods that consume spectral resources [4], [17]. While HetNets are part of LTE-Advanced, they are anticipated to play an even more central role in fifth generation (5G) networks. Further, in 5G much more back-end coordination between base stations is anticipated in the guise of Cloud Radio Access Networks or C-RANs [18]. Such back-end coordination is just the mechanism needed to assemble the passively sensed data that we require to estimate the network's interference environment.

We adopt the following set of notations. We use upper-case, e.g., X , and bold-face upper case, e.g., \mathbf{X} , to denote random variables and vectors, respectively. A vector without subscript consists of n elements, each corresponds to an AP, e.g., $\mathbf{X} := (X_1, X_2, \dots, X_n)$. Sets and events are denoted with calligraphic font (e.g., \mathcal{E}). The cardinality of a finite set \mathcal{V} is denoted as $|\mathcal{V}|$. A vector with a set as its subscript consists of the elements corresponding to the transmitters in the set, e.g., $\mathbf{Q}_{\mathcal{C}} := \{Q_c\}_{c \in \mathcal{C}}$.

The paper is organized as follows. In Section II we formulate the WLAN interference identification problem as a graph learning problem. We review the CSMA/CA (carrier sense multiple access with collision avoidance) protocol and propose a statistical model for a network using this protocol. In Section III we present our main results in the form of matching upper and lower bounds (up to constant factors) on the observation requirements for reliable estimation of both direct and hidden interference graph. We present an experimental study in Section IV that supports the theoretical analysis. The experiments are based on simulations of the traffic and protocol that incorporate more real-world effects than the models used to develop the theory. However, in the experiments the scaling behavior observed does match that predicted by theory. Concluding remarks are made in Section V. Most proofs are deferred to the appendices.

II. PROBLEM FORMULATION

In this section we present the problem setting. In Section II-A we present the important characteristics of the multiple-access protocol. In Section II-B we model the interference environment using a graph. In Section II-C we present

the estimation problem and sketch our algorithms. Finally, in Section II-D we present the statistical model and assumptions that underlie our analysis.

A. CSMA/CA protocol and ACK/NACK mechanism

We assume the wireless networks operates using a CSMA/CA-like protocol at the medium access control layer, e.g., [19]. The important characteristics of the protocol are as follows. When a node has a packet to send, it listens to the desired channel. If the channel is idle, it sends the packet. If the channel is busy, i.e., there exists an active transmitter within the listener’s carrier sensing range, the node waits for the end of that transmission, and then starts to contend for the channel. To contend, the node randomly chooses an integer w , uniformly distributed in the range $[0, W - 1]$, and then the node backs off for $w \times \tau$ seconds. The positive integer W represents the back-off window size, and τ is the duration of a time slot. If the channel is idle at the end of the node’s back-off period, it transmits its packet. The node that chooses the smallest back-off time wins the channel and transmits its packet. The other nodes wait for the next round of contention at the end of the transmission of this packet. According to this protocol, roughly speaking, the time axis can be partitioned into sessions, where each session consists of a contention period followed by a transmission period. Statistically, the random back-off mechanism allows every node equal access to the medium.

However, even if two APs are not within each other’s carrier sensing range, the transmission from one AP may still corrupt the signal received at clients of the other. This is the so-called “hidden terminal” problem. To identify this type of interference, additional information is needed. We assume that an ACK/NACK mechanism is used. Specifically, we assume that whenever an AP successfully delivers a packet to its destination, an ACK is fed back to acknowledge the successful transmission. If the AP does not receive the ACK after a period of time, it assumes that the packet was lost. The ACK/NACK mechanism enables the APs to detect collisions however they may occur. Throughout we assume that all ACKs are reliably received at the corresponding transmitters.

B. Interference Graph

We use a graph $G = (\mathcal{V}, \mathcal{E})$ to represent the interference among APs in the network. The node set \mathcal{V} represents the APs, and the edge set \mathcal{E} represents the pairwise interference among APs. An example of such a graph is depicted in Figure 1.

We partition \mathcal{E} into two subsets: *direct* interference \mathcal{E}_D and *hidden* interference \mathcal{E}_H . Direct interference occurs when two APs are within each other’s carrier sensing range. An example in Figure 1 is the AP pair (4, 5). Under the assumption that the carrier sensing range is the same for every AP, the edges in \mathcal{E}_D are *undirected*. However, as mentioned earlier, carrier sensing cannot resolve all of the collisions in the network. Hidden-terminal type interference is represented by the edges in \mathcal{E}_H . Such interference may be asymmetric and so the edges in \mathcal{E}_H are *directed*. In Figure 1 AP pairs (1, 2) and (3, 4) cannot detect each other. Yet, they can interfere with each

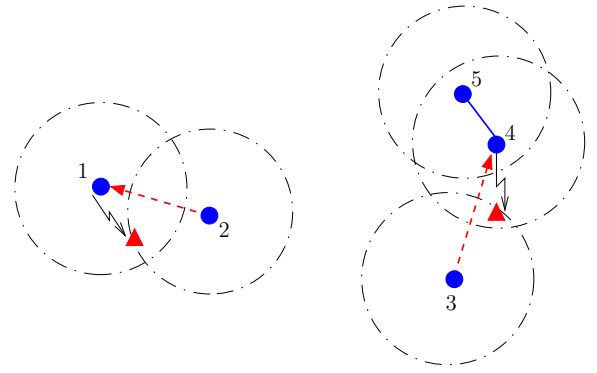


Fig. 1. System model with 5 APs. The edges connecting APs represent the interference between them. Solid line represents direct interference, dashed arrows represent hidden interference. Each circle represents the carrier sensing range of the AP at its center. Clients (represented by triangles) that are located in the intersection of the carrier sensing regions of a pair of APs may be subject to interference.

other’s clients since their carrier sensing ranges intersect. The affected clients would (roughly) lie in the intersection of the (roughly circular) carrier sensing ranges of the AP pair. Nodes 3 and 5 is an example of a pair of APs that do not interfere with each other (either directly or indirectly) since their carrier sensing ranges do not overlap.

C. Inference Problem and Algorithm

Our objective is to determine the edge set \mathcal{E} based on passive observations. We assume the existence of a central controller that, over a period of time, collects the transmission statuses of all APs and information on transmission successes (ACKs). The collected information during this *observation period* is the dataset we use to estimate the interference graph. Both enterprise-type WLANs and proposed architectures for 4G systems that involve combinations of macro plus pico-cells have such central controllers.

In this paper we consider *static channel states*. Specifically, we assume that whether or not a pair of APs can sense each other is fixed (deterministic) throughout the period of observation. For hidden interference, we also assume that the channel between each AP and all clients is also static. Further, if a transmission failure occurs it must have been caused by a collision with a packet transmitted by one of the other active APs.

We now outline the basic ideas underlying our algorithms. First, consider the direct interference environment, characterized by \mathcal{E}_D . Note that due to the use of carrier sensing in CSMA/CA, if two APs are within each other’s carrier sensing range, they will not transmit simultaneously. One can therefore infer that any pair of APs that transmit simultaneously during the observation period must not be able to hear each other. In other words, there is no *direct* interference between them. The algorithm starts with a full set of $\binom{|\mathcal{V}|}{2}$ candidate edges. Each time a simultaneous transmission is observed, the corresponding edge is removed. If the observation period is sufficiently long, all possible co-occurring transmission will be observed and the correct *direct* interference edge set \mathcal{E}_D will be recovered.

Next, consider the cases of hidden interference characterized by \mathcal{E}_H . Estimating this set is more involved and requires the collected ACK information. When a collision is detected at an AP, it implies that at least one of the other APs transmitting at the same time is interfering. The subset of APs transmitting at that time instance is a candidate set of hidden interferers for that AP. For each collision detected by the AP, another candidate subset is formed. The set of hidden interferers for that AP must have a non-empty intersection with *all* such candidate sets. When the observation period is sufficiently long, we show that the *minimum hitting set* [20] that intersects with all of the candidate subsets is the set of hidden interferers. The edge set \mathcal{E}_H can thus be recovered.

Our approaches to both problems were inspired by the PIE algorithms proposed in [5], [6]. For the direct interference problem, our approach is similar to PIE. Both rely on simultaneous transmissions to infer the interference graph. Our results provide the theoretical analysis and scaling behavior characterization that complement the empirical results of [5], [6]. Our approach to the hidden interferences problem is quite different from that taken in [5], [6]. While PIE uses a correlation based approach we use the hitting set approach described above. The hitting set approach results in more accurate estimation of the graph of hidden interferers, as elaborated in Sec. III-C.

D. Statistical Model

The graph $G_D = (\mathcal{V}, \mathcal{E}_D)$ represents the carrier sensing relationships among the APs. Specifically, if AP i and AP j are within each other's carrier sensing range, there is an edge between i, j , denoted as (i, j) . The existence of such an edge implies that AP i and AP j are close and the transmission of each can be observed by the other. An example in Figure 1 is the AP pair (4, 5). We term this "direct" interference and G_D the direct interference graph. We define \mathcal{N}_i to be the set of neighbors of AP i in $G_D = (\mathcal{V}, \mathcal{E}_D)$, and let $d_i = |\mathcal{N}_i|$.

Observations of the network activation pattern are taken each time epoch. We use $X_i(t) \in \{0, 1\}$ to denote the activation state of node i at time t : $X_i(t) = 1$ means that node i transmits; $X_i(t) = 0$ means that node i does not transmit. In general, $X_i(t)$ is determined by the traffic statuses and backoff times of the APs that compete for the same channel. We denote the traffic status of node i as $Q_i(t)$. $Q_i(t)$ is a Bernoulli random variable, and it equals one if node i has some content to send in slot t ; otherwise, it equals zero.

As mentioned, to infer the hidden interference we require information on transmission successes and failures. Define $Y_i(t) \in \{0, 1, \emptyset\}$ to be the feedback information received at AP i at the end of session t . $Y_i(t) = 1$ means that an ACK is received at AP i , indicating that the transmission in session t is successful; $Y_i(t) = 0$ means that the transmission has failed, caused by some simultaneous transmission(s); $Y_i(t) = \emptyset$ means that node i did not transmit in that session, i.e., $X_i(t) = 0$.

The graph $G_H = (\mathcal{V}, \mathcal{E}_H)$ represents the hidden interference among APs that cannot hear each other. This interference depends on the locations of the clients associated with each

AP and thus may not be symmetric. These edges are therefore *directed*. We define

$$p_{ij} = \mathbb{P}(Y_j(t) = 0 | X_i(t) = X_j(t) = 1, \mathbf{X}_{\mathcal{V} \setminus \{i, j\}}(t) = \mathbf{0}) \quad (1)$$

i.e., p_{ij} is the probability that, when i, j are isolated from the rest of the APs and $X_i(t) = X_j(t) = 1$, AP i interferes with AP j , causing transmission failure of AP j .

The p_{ij} capture the randomness in locations of the clients associated with each AP. An AP may interfere with only a subset of the clients of a neighboring AP. For example, in Fig. 1 AP 1 may interfere with a client of AP 2 that is halfway between the APs, but it likely will not interfere with a client on the far side of AP 2. Thus, which clients of an AP another AP interferes with depends on the locations of those clients. The value of p_{ij} represents the proportion of AP j 's clients that AP i interferes with. It can be interpreted as the probability that AP j communicates with a client located in the overlapped area of the carrier sensing ranges of APs i and j . Note that p_{ij} is not defined for $(i, j) \in \mathcal{E}_D$ since such pairs of APs are within each other's carrier sensing range and thus never transmit simultaneously. This is the case for AP 4 and AP 5 in Fig. 1.

Define $\mathcal{S}_j = \{(i, j) \in \mathcal{E}_H \mid i \in \mathcal{V}\}$ to be the hidden interferer set for AP j , i.e., the set of APs with $p_{ij} > 0$. We let $s_j = |\mathcal{S}_j|$. We point out that in general $\forall \mathcal{S} \subseteq \mathcal{V} \setminus \{i, j\}$,

$$p_{ij} \leq \mathbb{P}(Y_j(t) = 0 | X_i(t) = 1, X_j(t) = 1, \mathbf{X}_{\mathcal{S}} = \mathbf{0}), \quad (2)$$

i.e., p_{ij} is *less* than the probability that a collision occurs at AP j when both APs i and j are transmitting. This is because the collision at AP j may be caused by an active AP other than i , and AP i may just happen to be transmitting at the same time.

The complete interference graph $G = (\mathcal{V}, \mathcal{E})$ consists of both direct interference graph and hidden interference graph, i.e., $\mathcal{E} = \mathcal{E}_D \cup \mathcal{E}_H$. We note that $\mathcal{E}_D \cap \mathcal{E}_H = \emptyset$.

While we assume pairwise interference in our system model, the interference graph definition can be generalized to include more than just pairwise relationships. If certain types of interference can occur only when multiple APs are simultaneously transmitting, those APs form a virtual "super" interferer. We can include all possible super interferers as nodes in the inference graph without fundamentally changing the interference process.

We now state some statistical assumptions important in the development of our analytic results.

Assumption 1

- (0) APs are synchronized and the time axis is partitioned into synchronized sessions. We use $t = 1, 2, \dots$ to denote the indices of the observation sessions.
- (i) The traffic status $Q_i(t)$ are i.i.d. Bernoulli random variables with common parameter p , where $0 < p < 1$, for all $i \in \mathcal{V}$ and all $t \in \mathbb{Z}^+$. In other words, the $Q_i(t)$ are independent across transmitters and sessions: $\mathbb{P}(Q_i(t) = 1) = p$ for all i and t . APs competes for the channel at the beginning of session t if and only if $Q_i(t) = 1$.

- (ii) In the contention period at the beginning of each session, the backoff time $T_i(t)$ for competing APs are continuous i.i.d. random variables uniformly distributed over $[0, (W - 1) * \tau]$ and are statistically independent for all $i \in \mathcal{V}$ and all $t \in \mathbb{Z}^+$. W is a fixed positive integer, and τ is the duration of a time slot.
- (iii) For all $(i, j) \in \mathcal{E}_H$, there exists a constant p_{min} , $0 < p_{min} < 1$, s.t. $p_{ij} \geq p_{min}$.
- (iv) For all $i \in \mathcal{V}$, there exists an integer $d \in \mathbb{Z}^+$, s.t. $d_i \leq d$, i.e., the number of direct interferers of any AP is upper bounded by d .
- (v) For all $j \in \mathcal{V}$, there exists $s \in \mathbb{Z}^+$, s.t. $s_j \leq s$, i.e., the number of hidden interferers of any AP is upper bounded by s .

In the following, we use \mathcal{G}_d to denote the set of direct interference graphs consisting of n nodes and satisfying Assumption 1-(iv). Since whether an AP is a hidden interferer with respect to other APs depend on whether or not they can hear each other, the hidden inference graph of a network actually depend on its direct interference graph. Thus, for any given $G_D \in \mathcal{G}_d$, we define $\mathcal{H}_s(G_D)$ as the set of hidden interference graphs satisfying Assumption 1-(v).

Assumption 1-(0) is essential for our analysis. In practical WLANs, APs competing for the same channel are “locally” synchronized because of the CSMA/CA protocol. Assumption 1-(0) approximates the original “locally” synchronous system as a synchronized one. Since APs far apart on the interference graph have a relatively light influence on each other’s activation status, this assumption provides a good approximation of the original system and greatly simplifies our analysis.

Assumption 1-(i) ignores the time dependency and coupling effect of the traffic queue statuses of APs. This assumption is made to simplify the analysis. In a practical setting, the traffic queue status for a single AP is coupled from slot to slot, depending on whether the AP got access to the channel in the previous slot. The queue statuses of different APs can also be coupled (directly or indirectly) due to the common channels for which they compete. However, as long as the queues in the network are stable, their mixing time is finite from a queuing theory perspective. We can therefore always sample the network every T sessions so that the queue status dependency between two consecutive observation sessions are negligible when T is sufficiently large. This would add only a constant factor T to the required observation duration. However, we note that such an addition does not change our scaling results. Also, as indicated by our simulation results in Sec. IV, our algorithms do not require Assumption 1-(i) in order to function properly, so subsampling is, in fact, unnecessary.

The purpose of Assumption 1-(ii) is to ensure that with probability one no two adjacent nodes in $G_D = (\mathcal{V}, \mathcal{E}_D)$ have the same back-off time and therefore transmission collisions are avoided completely. Although in the CSMA/CA protocol, the backoff times are integer multiples of τ , this assumption is a reasonable approximation when W is a large integer. Roughly speaking, the probability that two adjacent nodes

in G_D choose the same backoff time under the CSMA/CA protocol is upper bounded by $1/W^2$. Given that the number of edges in G_D is upper bounded by $nd/2$, and through application of the union bound, the probability that a collision happens is upper bounded by $\frac{nd}{2W^2}$. Further, asynchrony of AP operations in real networks make the probability of collision even smaller. We thus make Assumption 1-(ii) to simplify our analysis without compromising much in terms of accuracy. Finally, we note that this assumption is applied only for analytical purposes and is not applied in the experimental section where we observe the predicted scaling laws under a more realistic simulation of protocol operations. We comment that we did analyze a model wherein collisions are allowed to occur, and we did extend our interference estimation algorithm to handle this case. We are not able to include those results herein due to space constraints, but they can be seen in the online version of the paper [21].

The first two assumptions guarantee that the joint distribution of $X_i(t)$ s and $Y_i(t)$ s is independent and identical across t . Therefore, in the analysis hereafter we ignore the time index and focus on the distribution of X_i s and Y_i s in a single observation.

Regarding the last three assumptions, assumption 1-(iii) defines a lower bound on the level of interference of interest. The final assumptions, (iv) and (v), model the fact that the interference graph will be sparse because of the widespread spatial distributions natural to the large-scale wireless networks of interest.

III. MAIN RESULTS

In this section we present our main results. We break the overall problem into four subproblems. In Section III-A we provide an achievable upper bound on the number of observations required to infer the directed interference edge set \mathcal{E}_D . In Section III-B we present a matching lower bound on the number of observations required to infer \mathcal{E}_D . In Section III-C we provide an achievable upper bound on the number of observations required to infer the hidden interference edge set \mathcal{E}_H . Finally, in Section III-D we present a lower bound on the number of observations required to infer \mathcal{E}_H .

A. An Upper Bound for Determining $G_D = (\mathcal{V}, \mathcal{E}_D)$

In this section, we formalize the algorithm sketched in Section II-C for estimating $G_D = (\mathcal{V}, \mathcal{E}_D)$ and present an analysis thereof. In the static setting, for any $(i, j) \in \mathcal{E}_D$, APs i and j can always sense each other’s transmissions. For any AP pair $(i, j) \notin \mathcal{E}_D$, the APs can never detect each other’s transmissions.

Say that a sequence of transmission patterns $\mathbf{X}(1), \mathbf{X}(2), \dots, \mathbf{X}(k)$ is observed. Due to the use of the CSMA/CA protocol and the continuous back-off time of Assumption 1-(ii), any pair of APs active in the same slot must not be able to hear each other. Thus, there is no edge in $G_D = (\mathcal{V}, \mathcal{E}_D)$. In other words, given an observation \mathbf{X} , for any i, j with $X_i = X_j = 1$, we know that $(i, j) \notin \mathcal{E}_D$.

Based on this observation, the algorithm starts at $t = 1$ with a fully connected graph connecting the n APs with $\binom{|\mathcal{V}|}{2} =$

$n(n-1)/2$ edges. For each transmission pattern \mathbf{X} observed, we remove all edges (i, j) s.t. $X_i = X_j = 1$. Our first result quantifies the number of observations k required to eliminate, with high probability, all edges not in \mathcal{E}_D , thereby recovering the underlying interference graph G_D . In Appendix A we show the following result:

Theorem 1 *Let $\delta > 0$, and let*

$$k \geq \frac{1}{\log \frac{1}{1-p^2/(d+1)^2}} \left(\log \binom{n}{2} + \log \frac{1}{\delta} \right). \quad (3)$$

Then, with probability at least $1-\delta$, the estimated interference graph $\hat{G}_D = (\mathcal{V}, \hat{\mathcal{E}}_D)$ is equal to G_D for any $G_D \in \mathcal{G}_d$ after k observations.

The idea of the proof is first to lower bound the probability that two nonadjacent APs i, j never transmit simultaneously in k observations. Then, by taking a union bound, an upper bound on the required k is obtained.

Remark: If $p^2/d^2 \ll 1$ the scaling on k in the theorem simplifies to $O(d^2 \log n)$. We see this by noting that if $p^2/d^2 \ll 1$ then $-\log(1-p^2/(d+1)^2)$ is well approximated by p^2/d^2 and $\log \binom{n}{2}$ scales as $\log n$. Most networks of interest will fall in this regime, e.g., if $p = 0.5$ and $d = 3$ then p^2/d^2 will be a good approximation of $-\log(1-p^2/(d+1)^2)$. This sort of scaling in p and d can easily be believed to be the best we can hope for when passive estimation is employed. This follows because if two non-interfering APs never transmit simultaneously, their behavior is the same as if they were within each other's carrier sensing range. Thus, we cannot determine whether or not there is an edge between them. Since each transmitter competes with its neighbors, the probability that it gets the channel is roughly p/d . Thus, it takes about d^2/p^2 snapshots to observe two non-interfering APs active at the same time. Since there are about n^2 such pairs in the network, an application of the union bound yields the factor $\log n$.

B. A Minimax Lower Bound for Determining $G_D = (\mathcal{V}, \mathcal{E}_D)$

We now provide a minimax lower bound on the number of observations needed to recover the direct interference graph $G_D = (\mathcal{V}, \mathcal{E}_D)$. Denoting the estimated graph as $\hat{G}_D = (\mathcal{V}, \hat{\mathcal{E}}_D)$ we prove the following result in Appendix B.

Theorem 2 *For any α , $0 < \alpha < 1/8$, if $n \geq 7$, $2 \leq d \leq (3n - \sqrt{n^2 + 16n})/4$, and*

$$k \leq \frac{\alpha d^2}{\left(2 + \frac{1}{1-p}\right)} \log n,$$

then,

$$\begin{aligned} & \min_{\hat{G}_D \in \mathcal{G}_d} \max_{G_D \in \mathcal{G}_d} \mathbb{P}(\hat{G}_D \neq G_D; G_D) \\ & \geq \frac{\sqrt{n}}{1 + \sqrt{n}} \left(1 - 2\alpha - \sqrt{\frac{2\alpha}{\log n}} \right). \end{aligned} \quad (4)$$

The approach to deriving this result is as follows. We construct a set of M maximum-degree d graphs. We construct

the set so that the graphs in the set are very similar to each other. This makes it hard to distinguish between them. For each graph in the set the statistical assumptions of Section II-D induce a distribution on the observed transmission patterns. Given k observed transmission patterns we consider the M -ary hypothesis test to detect the underlying graph. As the size of the candidate set for the original estimation problem is much greater than M , this test will be easier than the original problem. Therefore, a lower bound for this test will also lower bound the original estimation problem. Since for each graph we know the distribution of patterns, we can lower bound the probability of error for this hypothesis test using the Kullback-Leibler divergence between each pair of induced distributions.

Remark: We note that the RHS of (4) is bounded away from zero, and $\frac{\sqrt{n}}{1+\sqrt{n}} \geq \frac{\sqrt{3}}{1+\sqrt{3}}$ for $n \geq 3$. Therefore, for any $\delta < \frac{\sqrt{3}}{1+\sqrt{3}}$, we can always find a positive α so that $\min_{\hat{G}_D} \max_{G_D} \mathbb{P}(\hat{G}_D \neq G_D; G_D) \geq \delta$. Then, the number of observations required to detect the correct underlying graph with probability $1 - \delta$ is $\Omega(d^2 \log n)$ which, as discussed earlier, when $p^2/d^2 \ll 1$, is the same order as the upper bound in Theorem 1. Therefore, the estimation method based on pairwise comparison is asymptotically optimal when d is large.

C. An Upper Bound for Determining $G_H = (\mathcal{V}, \mathcal{E}_H)$

We now present our results on inferring the hidden interference graph $G_H = (\mathcal{V}, \mathcal{E}_H)$. We observe $\mathbf{X}(1), \dots, \mathbf{X}(k)$ and $\mathbf{Y}(1), \dots, \mathbf{Y}(k)$. When the transmission of AP j fails (indicated by the feedback $Y_j = 0$) the failure must have been caused by collision with a transmission from one of the active APs in \mathcal{S}_j . However, as there may be multiple hidden interferers, there may be no single AP that is always transmitting when $Y_j = 0$. Complicating the situation is the fact that an AP that transmits regularly when $Y_j = 0$ may not be a hidden interferer at all. This is because the transmission status of an AP can be strongly positively correlated (because of CSMA/CA) with one or more non-interferers. We first illustrate the types of statistical dependencies we need to address before presenting our algorithm.

First, consider a scenario where AP 1, AP 2, and AP 3 lie in the direct interference range of AP l , i.e., APs 1, 2, and 3 are all in \mathcal{N}_l . Further assume that there is no direct interference between 1, 2, and 3. The transmission of any of these three APs will suppress the transmission of AP l and thus increase the (conditional) probability of transmission of the other APs in \mathcal{N}_l . Thus, the activation statuses of 1, 2, 3 are positively correlated. Now say that APs 1, 2 are both hidden interferers for AP m , $m \notin \{1, 2, 3, l\}$. Then, even though transmissions of AP 3 may be correlated with transmission failures of AP m , due to the positive correlation statuses of 1, 2, 3, AP 3 may not be a hidden interferer for node m . One possible scenario is that $\mathbb{P}(Y_m = 0 | X_3 = 1, X_m = 1)$ may be even greater than $\mathbb{P}(Y_m = 0 | X_1 = 1, X_m = 1)$ or $\mathbb{P}(Y_m = 0 | X_2 = 1, X_m = 1)$. The upshot is that correlation-based approaches to determining hidden interferers, such those adopted in [5], [6], may not be able distinguish true interferers from non-interferers. To

address these issues we propose the following approach, based on *minimum hitting sets*.

First, given k observations, define

$$\mathcal{K}_j(k) = \{t \in \{1, 2, \dots, k\} \mid Y_j(t) = 0\}$$

to be the sessions in which AP j 's transmissions fail. For each j and each t define the set of candidate hidden interferers as

$$\mathcal{S}_j^t = \{i \in \mathcal{V} \mid i \neq j, X_i(t) = 1\}.$$

We will be interested only in t such that $t \in \mathcal{K}_j(k)$. Our estimator of the set of hidden interferers $\hat{\mathcal{S}}_j(k)$ is the *minimum hitting set* of the candidate interferer sets $\{\mathcal{S}_j^t\}_{t \in \mathcal{K}_j(k)}$:

$$\hat{\mathcal{S}}_j(k) = \arg \min_{\mathcal{S} \subseteq \mathcal{V}} \{|\mathcal{S}| \mid \mathcal{S} \cap \mathcal{S}_j^t \neq \emptyset, \forall t \in \mathcal{K}_j(k)\},$$

where, if there are multiple minimizers, one is selected at random.

In general, a minimum hitting set is defined as follows:

Definition 1 (Minimum Hitting Set) *Given a collection of subsets of some alphabet, a set which intersects all subsets in the collection in at least one element is called a ‘‘hitting set’’. A ‘‘minimum’’ hitting set is a hitting set of the smallest size.*

Given k observations, our algorithm determines the minimum hitting set $\hat{\mathcal{S}}_j(k)$ of $\{\mathcal{S}_j^t \mid t \in \mathcal{K}_j(k)\}$ for each $j \in \mathcal{V}$. To get a sense of the usefulness of the concept of the minimum hitting set when considering hidden interferers, consider when a single AP j has two hidden interferers, both of which are active for all $t \in \mathcal{K}_j(k)$. Since we look for the *minimum* hitting set only one of these would be included in the graph estimate. However, if we wait sufficiently long, we will experience a pair of transmissions in which each of these two hidden interferers is solely active. At that point both will be included in the graph estimate. In contrast, while if we don't require the *minimum* hitting set to be our estimate both hidden interferers might be included in our estimated graph earlier, so might be other nodes that are non-interfering but happen always to be active in conjunction with various distinct hidden interferers.

The following theorem provides an upper bound on the number of observations required so that $\hat{\mathcal{S}}_j(k) = \mathcal{S}_j$ for every AP $j \in \mathcal{V}$ with high probability. Once the estimated minimum hitting set $\hat{\mathcal{S}}_j(k)$ is obtained, the estimated hidden interference graph \hat{G}_H is constructed by adding a directed edge from each AP in $\hat{\mathcal{S}}_j(k)$ to AP j , i.e.,

$$\hat{\mathcal{E}}_H = \bigcup_{j \in \mathcal{V}} \{(i, j) \mid i \in \hat{\mathcal{S}}_j(k)\}.$$

The following theorem is proved in Appendix C.

Theorem 3 *Let $\delta > 0$, and let*

$$k \geq \frac{1}{\log \frac{1}{1 - \frac{p^2(1-p)^s p_{\min}}{(d+1)^2}}} \left(\log(ns) + \log \frac{1}{\delta} \right)$$

Then, with probability at least $1 - \delta$, \hat{G}_H equals G_H for any given $G_D \in \mathcal{G}_d$ and $G_H \in \mathcal{H}_s(G_D)$.

The approach taken in the proof can be summarized as follows. For every AP j , we first upper bound the probability that the minimum hitting set obtained after k observations is not equal to the true minimum hitting set. This is equal to the probability that there exists at least one AP $i \in \mathcal{S}_j$ that is not included in $\hat{\mathcal{S}}_j$. As mentioned above, this will happen (at least) if two hidden interferers happen to both be on in all $t \in \mathcal{K}_j(k)$. By taking the union bound across all possible i and j , we obtain an upper bound on k . The upper bound $k = O\left(\frac{d^2}{p^2(1-p)^s p_{\min}} \log n\right)$ when $\frac{p^2(1-p)^s p_{\min}}{d^2} \ll 1$.

In general, finding the minimum hitting set is NP-hard [20]. However, under the assumption that the maximum possible number of hidden interferers $s \ll n$, the total number of nodes in the network, the minimum hitting set can be solved for in polynomial time. This is a regime appropriate to the large-scale wireless networks of interest in this paper. First we use the algorithm of Section III-A to identify G_D . Next, we consider each AP in turn. For AP j , we test every subset of nonadjacent APs in G_D (not including AP j) to determine whether it is a hitting set of $\{\mathcal{S}_j^t \mid t \in \mathcal{K}_j(k)\}$. Since the number of hidden interferers $s_j \leq s$, we start with the smallest possible hitting sets, i.e., $s_j = 1$. We increment the size of the testing subset by one, until a hitting set is achieved. In this way we find the minimum hitting set for the given $\{\mathcal{S}_j^t \mid t \in \mathcal{K}_j(k)\}$.

The worst situation for this incremental approach will be when s_j is as large as possible. By Assumption 1-(v) $s_j \leq s$. Recalling that d_j is the number of direct interferers (which can be eliminated from consideration), in this case the maximum number of subsets we must test is

$$\sum_{i=1}^s \binom{n - d_j - 1}{i} = \beta_3 (n - d_j - 1)^s$$

for some bounded constant β_3 . In other words, the number of subsets we need to test is upper bounded by $O(n^s)$ [22].

D. A Minimax Lower Bound for Determining $G_H = (\mathcal{V}, \mathcal{E}_H)$

Finally, we provide a lower bound on the number of observations required to recover the underlying hidden interference graph $G_H = (\mathcal{V}, \mathcal{E}_H)$. In Appendix D we prove the following theorem.

Theorem 4 *Assume $s \geq 2$. For any $c_1, c_2 > 0$ s.t.*

$$d + 1 \leq c_1 n, \quad s - 1 \leq c_2 n, \quad 2c_1 + c_2 < 1. \quad (5)$$

If

$$k \leq \frac{\log \frac{1}{2c_1(\frac{1}{2c_1+c_2}-1)n}}{\left(\frac{1-(1-p)^{d+1}}{d+1}\right)^2 (1-p)^{s-1} \log(1-p_{\min})}$$

then for any $\alpha, 0 < \alpha < 1/8$,

$$\min_{\hat{G}_H \in \mathcal{H}_s(G_D)} \max_{G \in \mathcal{G}_d \times \mathcal{H}_s(G_D)} \mathbb{P}(\hat{G}_H \neq G_H; G) \geq \frac{\sqrt{2c_1(\frac{1}{2c_1+c_2}-1)n}}{1 + \sqrt{2c_1(\frac{1}{2c_1+c_2}-1)n}} \left(1 - 2\alpha - \sqrt{\frac{2\alpha}{\log(2c_1(\frac{1}{2c_1+c_2}-1)n)}} \right).$$

The first two conditions expressed in (5) ensure that the maximum number of direct interferers d , and the bound on the number of hidden interferers s , both scale at most linearly in n . The third constraint places a limit on the joint scaling. The approach to deriving this result is the same as the one we followed for the proof of Theorem 2. We reduce the original problem to an M -ary hypothesis test and show that, asymptotically, the lower bound has the same order as the upper bound.

Remark: Since the distribution of \mathbf{Y} depends on the underlying direct interference graph as well as on the hidden interference graph, the lower bound is over all possible interference graphs G . As we discussed after Theorem 2, for a sufficiently small positive number δ , we can always find a positive α so that $\min_{\hat{G}_D} \max_{G_D} \mathbb{P}(\hat{G}_D \neq G_D; G_D) \geq \delta$. Then, as d increases, the number of observations required to detect the correct underlying graph with probability $1 - \delta$ is $\Omega\left(-\frac{d^2}{\log(1-p_{\min})(1-p)^{s-1}} \log n\right)$. Since $\log(1 - p_{\min})$ can be approximated as $-p_{\min}$ when p_{\min} is small, the lower bound is of the same order as the upper bound provided in Theorem 3. Therefore, the bounds are tight and our hitting-set based algorithm is asymptotically optimal.

IV. SIMULATION RESULTS

In this section we present simulation results with the aim of verifying the applicability of the theory developed earlier. We use our algorithms to infer interference graphs based on traffic traces collected from a simulated wireless network that operates according to the IEEE 802.11 CSMA/CA protocol. In comparison to the statistical assumptions made to derive the theoretical learning bounds in this paper, the simulations mimic real-world wireless networks much more closely.

We comment on the specific differences between the following simulations and the assumptions made in the analyses of Section III. First, the nodes in the simulations operate in an asynchronous fashion instead of working synchronously. Therefore, the synchronized session model of Assumption 1-(0) does not hold in the simulations. Second, we introduce a queue at the MAC layer for each AP to store data packets that haven't yet been delivered. A packet stays in the MAC queue until it has been successfully received at the destination client or has been dropped (after two retransmission attempts). Therefore, the independent traffic status assumption made in Assumption 1-(i) does not hold. Third, the backoff time for each AP is not continuous but is an integer multiple of a slot time (20×10^{-6} s). This means that two APs within each other's carrier sensing range have a (small) probability of colliding, especially when the window length W is short. These differences break the i.i.d. assumption regarding the joint distribution of $X_i(t)$ and $Y_i(t)$ across time. As we will see, despite the added complexities of this more realistic simulation environment, the behavior we observe closely matches the quantitative predictions made by the theory.

The specific setup for the simulations is as follows. Access points and clients are deployed over a rectangular area that can be partitioned into square cells 50m on a side. An AP is placed uniformly at random within each cell, while a client

is placed at the center of the cell. Each client is associated with the nearest AP. We choose the network topology in this manner to ensure the randomness of the corresponding interference graph while still maintaining a relatively balanced traffic intensity across the network. Because there is a single client associated with each AP, in these simulations we are essentially evaluating the interference between AP-client links, similar to the setup in [6]. The locations of APs and clients are fixed throughout the period of observation.

At the MAC layer, we generate an independent downlink traffic flow for each client according to a Poisson process of λ packet arrivals per slot time. Packets payloads are all identical, of 1000 bits each. We set the contention window size to be 16 slot times.

At the PHY layer, we employ the log-distance path loss model. In this model, received power (in dB) at distance l (in meters) from the transmitter is given by:

$$\Gamma(l) = \Gamma(l_0) - 10\eta \log(l/l_0) + X_\sigma. \quad (6)$$

In the above, $\Gamma(l_0)$ is the signal strength at the reference distance l_0 from the transmitter, η is the path loss exponent, and X_σ represents a Gaussian random variable with zero mean and variance σ^2 in dB. We choose l_0 to be 1 km, σ^2 to be 5dB, and η to be 4. We also assume that the "shadowing" (represented by X_σ) between any AP and AP-client pair is fixed throughout the period of observation. Thus the underlying interference graph is constant within the period of observation.

We fix the transmission rate to be 5Mbps and the transmission range for APs to be 37.5m. The transmit power and corresponding received SNR threshold are selected to ensure successful transmissions within the transmission range.

We first study the direct interference estimation algorithm of Section III-A. We fix the carrier sensing range for the APs to be 60m. We vary the size of the network where the network consists of an array of square cells. For each network size, we randomly generate ten topologies, i.e., AP positions are randomly chosen. For each of the ten topologies, we use our algorithm to recover G_D under different (randomly generated) traffic traces.

In Fig. 2 we report the average duration of the observation period required to recover the direct interference graph for each network size. The average time is plotted versus the number of APs for four different traffic intensities $\lambda \in \{0.002, 0.003, 0.004, 0.005\}$. We observe that although, as discussed above, the assumptions we adopted to derive the scaling laws do not hold in the simulation, the duration required to identify the network scales in the predicted, sub-linear (logarithmic), manner in network size n . This is consistent with the scaling predicted by Thm. 1. The necessary observation time decreases as traffic intensity increases, also as predicted by the theory.

In Fig. 3 we study the average observation time required to recover the direct interference graph as a function of maximum degree d for a fixed network size. We conduct the experiment as follows. We fix the network size to be 4×15 cells and randomly generate topologies (AP and client positions). For each randomly generated topology, we vary the carrier

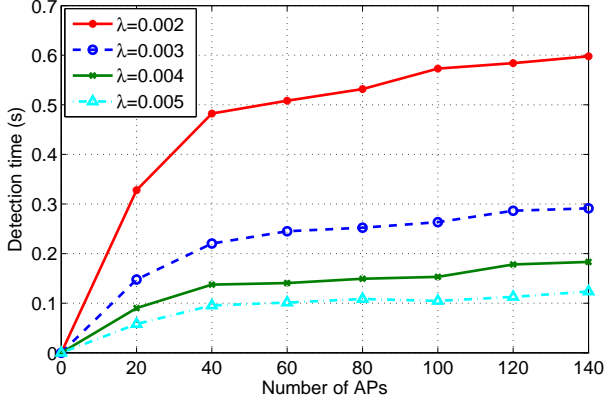


Fig. 2. The observation duration required to recover the direct interference graph for networks with a maximum of $d = 6$ direct interferers and $s = 1$ hidden interferer per node, plotted as a function of the number of APs in the network.

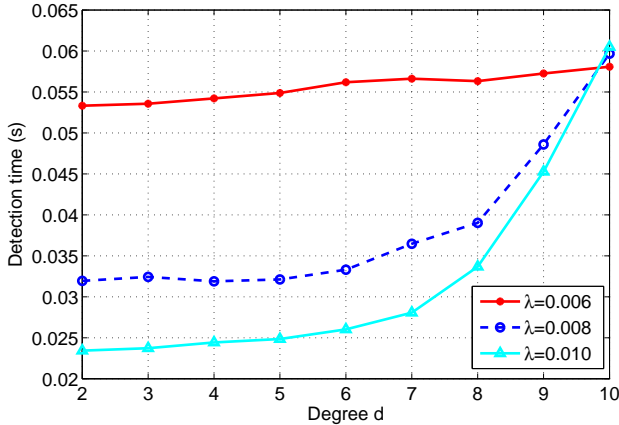


Fig. 3. The observation duration required to recover the direct interference graph for networks composed of 4×15 cells, plotted as a function of d , the maximum number of direct interferers.

sensing range: 25m, 35m, 45m, 55m, 65m, 75m. We check the maximum degree d (the number of direct interference edges per node) for each topology. We select ten topologies for each d varying from 2 to 10. We then simulate the network in each case. We plot the average observation time required to recover G_D as a function of the maximum degree d .

Figure 3 demonstrates that in the heavy traffic regime ($\lambda \in \{0.008, 0.01\}$) the scaling is super-linear (quadratic) in d , as predicted by the theory. However, in a lighter traffic regime ($\lambda = 0.006$), the super-linear scaling is not obvious. The reason for the different behavior as a function of traffic intensity is as follows. In the heavy traffic regime the probability that a node competes for the channel does not increase as d increase since its queue is almost always non-empty even when the node does not get to transmit. This makes the predicted quadratic scaling in d easy to see. In contrast, in a sufficiently light traffic regime, the marginal probability that a node competes for the channel increases as d increases, due to the time-dependency of the queue state. Since the p in Thm. 1 is now a function of d , it essentially compensates for the quadratic scaling in d . Thus, the super-linear (quadratic)

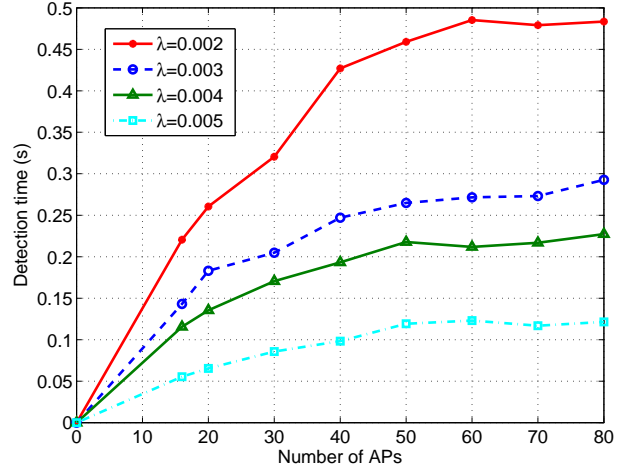


Fig. 4. The observation duration required to recover the hidden interference graph for networks with a maximum of $d = 6$ direct interferers and $s = 1$ hidden interferer per node, plotted as a function of the number of APs in the network.

scaling effect is not easily discernible in this regime.

In Fig. 4 we consider the hidden interference graph estimation problem. We plot, as a function of network size, the observation duration required to identify the minimum hitting set correctly for each node and to recover the hidden interference graph. The same simulation conditions hold as were described in the discussion of Fig. 2. For this algorithm we again observe that the necessary observation duration scales sub-linearly (logarithmically) in network size n .

In Fig. 5 we examine the dependence of the necessary observation duration on s , the number of hidden interferers per node. In these simulations we fix the network size to be 4×15 cells and the carrier sensing range to be 60m. We randomly generate topologies with fixed $d = 6$, and let s vary from 1 to 4. The required observation duration is plotted as a function of s . We see that the observation duration increases super-linearly as s increases, which is consistent with the predictions of Thm. 3.

V. CONCLUSIONS

In this paper, we propose passive interference learning algorithms and analyze their learning bounds. We first upper bound the number of measurements required to estimate the direct interference graph. Then, we provide a minimax lower bound by constructing a sequence of networks and transforming it into an M -ary hypothesis test. The lower bound matches the upper bound (up to a constant). Thus, the bound is tight and the algorithm is asymptotically optimal. We then analyze the estimation of the hidden interference graph estimation based on the minimum hitting set algorithm. We provide matching lower and upper bounds following an approach similar to that employed for the direct interference graph. We also present an experimental study that lends support to the theoretical analysis.

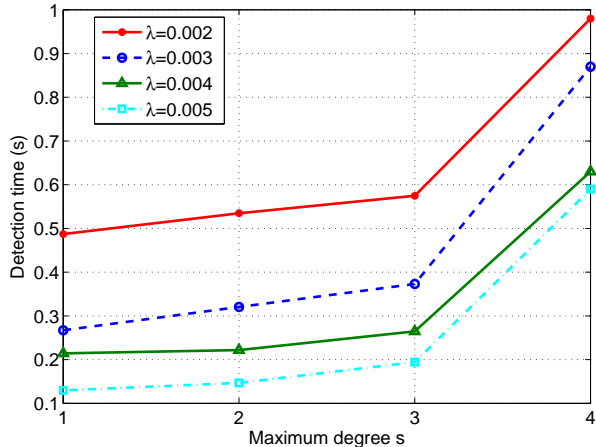


Fig. 5. The observation duration required to recover the hidden interference graph for networks composed of 4×15 cells, with a maximum of $d = 6$ direct interferers per node, plotted as a function of s , the maximum number of hidden interferers per node.

APPENDIX

A. Proof of Theorem 1

Consider any two nonadjacent nodes i, j in $G_D = (\mathcal{V}, \mathcal{E}_D)$. Let $\mathcal{N}_{ij} = \mathcal{N}_i \cup \mathcal{N}_j$, and $\mathcal{N}_{i \setminus j} = \mathcal{N}_i \cap \mathcal{N}_j^c$.

Under the CSMA/CA protocol, transmitter i only contends for the channel when $Q_i = 1$. For ease of exposition, in this proof, we assume that every transmitter will first choose a random backoff time at the beginning of each session, whether or not its queue is non-empty. However, only APs with $Q_i = 1$ will actually compete for the channel. A transmitter with $Q_i = 0$ will not transmit even if it has the shortest backoff time.

Define $T_{\mathcal{N}_i}$ as the minimum back-off time of the nodes in the set \mathcal{N}_i . Then,

$$\begin{aligned} \mathbb{P}(T_i < T_{\mathcal{N}_i}, T_j < T_{\mathcal{N}_{j \setminus i}}) &= \frac{\binom{|\mathcal{N}_{ij}|+2}{|\mathcal{N}_i|+1} \cdot |\mathcal{N}_i|! \cdot |\mathcal{N}_{j \setminus i}|!}{(|\mathcal{N}_{ij}|+2)!} \quad (7) \\ &= \frac{1}{(|\mathcal{N}_i|+1)(|\mathcal{N}_{ij}|-|\mathcal{N}_i|+1)} \\ &\geq \frac{1}{(d_i+1)(d_j+1)} \geq \frac{1}{(d+1)^2}. \end{aligned}$$

The logic underlying (7) is as follows. Consider nodes i, j and their neighbors. There are $|\mathcal{N}_{ij}|+2$ nodes in total, and there are $(|\mathcal{N}_{ij}|+2)!$ orderings of their back-off times. Among these orderings, $\binom{|\mathcal{N}_{ij}|+2}{|\mathcal{N}_i|+1} \cdot |\mathcal{N}_i|! \cdot |\mathcal{N}_{j \setminus i}|!$ orderings correspond to $T_i < T_{\mathcal{N}_i}, T_j < T_{\mathcal{N}_{j \setminus i}}$. Such an ordering can be obtained in the following way. Suppose these $|\mathcal{N}_{ij}|+2$ nodes are ordered according to their back-off times. Node i and its neighbors take $|\mathcal{N}_i|+1$ positions in the ordering. There are $\binom{|\mathcal{N}_{ij}|+2}{|\mathcal{N}_i|+1}$ different combinations of these positions. Since $T_i < T_{\mathcal{N}_i}$, node i takes the first position out of the chosen $|\mathcal{N}_i|+1$ positions, the remaining $|\mathcal{N}_i|$ positions are for its neighbors. This results in $|\mathcal{N}_i|!$ orderings for each combinations of positions. Node j and the nodes in $\mathcal{N}_{j \setminus i}$ take the rest of the positions, where node j takes the first. This gives the factor $|\mathcal{N}_{j \setminus i}|!$.

When $T_i < T_{\mathcal{N}_i}$ and $Q_i = 1$ then, based on the protocol,

node i gets the channel and thus $X_i = 1$. At the same time, transmissions from all nodes in \mathcal{N}_i are suppressed. Therefore, for node j , if $T_j < T_{\mathcal{N}_{j \setminus i}}$ and $Q_j = 1$, node j also gets a channel. Thus, we have $X_i = X_j = 1$. Since all other scenarios result in $X_i = X_j = 1$, we have the following

$$\begin{aligned} \mathbb{P}(X_i = 1, X_j = 1) &\geq \mathbb{P}(T_i < T_{\mathcal{N}_i}, T_j < T_{\mathcal{N}_{j \setminus i}}, Q_i = 1, Q_j = 1) \\ &= \mathbb{P}(T_i < T_{\mathcal{N}_i}, T_j < T_{\mathcal{N}_{j \setminus i}}) \mathbb{P}(Q_i = 1, Q_j = 1) \\ &\geq \frac{p^2}{(d+1)^2} \quad (8) \end{aligned}$$

and

$$\begin{aligned} \mathbb{P}(\text{edge } (i, j) \text{ is not removed by a single observation } \mathbf{X}) &= 1 - \mathbb{P}(X_i = 1, X_j = 1) \leq 1 - \frac{p^2}{(d+1)^2}. \end{aligned}$$

Define \mathcal{A}_{ij} as the event that edge (i, j) is not removed after k observations. Then, the probability that, after k observations, the graph cannot be identified successfully is

$$\mathbb{P}(\hat{G}_D \neq G_D) = \mathbb{P}(\cup_{(i,j) \notin \mathcal{E}_D} \mathcal{A}_{ij}) \leq \binom{n}{2} \left(1 - \frac{p^2}{(d+1)^2}\right)^k.$$

The inequality follows from the fact that the number of nonadjacent pairs in $G_D = (\mathcal{V}, \mathcal{E}_D)$ is upper bounded by $\binom{n}{2}$. Under the assumption that $d \ll n$, this is a good approximation for the nonadjacent pairs in G_D .

B. Proof of Theorem 2

Recall that \mathcal{G}_d is defined as the set of graphs consisting of n nodes that have maximum degree d . We are going to construct a collection of $M+1$ graphs $\{G_{D0}, G_{D1}, \dots, G_{DM}\}$ where $G_{Di} \in \mathcal{G}_d$ for all i . We denote the distribution of transmission patterns $\mathbf{x} \in \{0, 1\}^n$ for each of these graphs as $P_0(\mathbf{x}), P_1(\mathbf{x}), \dots, P_M(\mathbf{x})$, respectively. Define $\mathbb{P}(\mathcal{A}; G_D)$ to be the probability of event \mathcal{A} occurring where the underlying direct interference graph is $G_D \in \mathcal{G}_d$. A metric of interest is the edit or ‘‘Levenshtein’’ distance between a pair of graphs. This is the number of operations (i.e., addition/removal of one edge) needed to transform one graph into the other. We denote the Levenshtein distance between G_{Di} and G_{Dj} as $D_L(G_{Di}, G_{Dj})$. Then, we apply Theorem 2.5 in [23] to obtain the lower bound. We restate the theorem in terms of our problem as follows.

Theorem 5 (adapted from [23]) Let $k \in \mathbb{Z}^+$, $M \geq 2$, $\{G_{D0}, \dots, G_{DM}\} \in \mathcal{G}_d$ be such that

- (i) $D_L(G_{Di}, G_{Dj}) \geq 2r$, for $0 \leq i < j \leq M$, where D_L is the Levenshtein Distance,
- (ii) $\frac{k}{M} \sum_{i=1}^M D_{KL}(P_i || P_0) \leq \alpha \log M$, with $0 < \alpha < 1/8$.

Then

$$\begin{aligned} \inf_{\hat{G}_D \in \mathcal{G}_d} \sup_{G_D \in \mathcal{G}_d} \mathbb{P}(D_L(\hat{G}_D, G_D) \geq r; G_D) &\geq \inf_{G_D \in \mathcal{G}_d} \max_i \mathbb{P}(D_L(\hat{G}_D, G_{Di}) \geq r; G_{Di}) \\ &\geq \frac{\sqrt{M}}{1 + \sqrt{M}} \left(1 - 2\alpha - \sqrt{\frac{2\alpha}{\log M}}\right) > 0. \end{aligned}$$

In the following, we apply Theorem 5 to obtain a lower bound on k . We next construct the $M + 1$ graphs $\{G_{D0}, G_{D1}, \dots, G_{DM}\}$ to satisfy the two conditions – (i) and (ii) – of Theorem 5. We first construct G_{D0} and characterize $P_0(\mathbf{x})$. Then, we construct the rest of the M graphs by perturbing G_{D0} . These graphs will be symmetric in the sense that $D_{KL}(P_i||P_0)$ will be the same for $1 \leq i \leq M$. We calculate $D_{KL}(P_1||P_0)$ and then lower bound the number of observations k required to determine the interference graph with high probability.

1) G_{D0} and its transmission pattern distribution $P_0(\mathbf{x})$: Assume $d \geq 2$. We let graph G_{D0} consist of $\lceil n/d \rceil$ disconnected cliques. The first $\lfloor n/d \rfloor := m_0$ cliques are each a fully connected subgraph of d nodes, as shown in Fig. 6. The remaining nodes – if n/d is not integer – form a clique of size less than d . Our analysis focuses on the first m_0 cliques.

Denote \mathcal{C}_m as the set of nodes in the m th clique and let $\mathbf{X}_{\mathcal{C}_m}$ be the restriction of the transmission pattern \mathbf{X} to the nodes in the clique ($\mathbf{X}_{\mathcal{C}_m}$ is a set of subvectors, $m = 1, 2, \dots, m_0$ that partition \mathbf{X}). Define \mathbf{e}_i as the unit vector of dimension d whose i th element is one. Define $\mathbf{0}$ to be the all-zeros vector of length d . Due to the fully connected structure of the cliques, no more than one node in any \mathcal{C}_m can transmit at any time. We denote the set of all feasible transmission patterns for clique m as $\mathcal{X}_m := \{\mathbf{0}, \mathbf{e}_1, \dots, \mathbf{e}_{|\mathcal{C}_m|}\}$. If $\mathbf{X}_{\mathcal{C}_m} = \mathbf{0}$, then no node in \mathcal{C}_m is transmitting in that session. For each individual clique, this event happens only when none of the nodes in that clique has traffic to send, i.e.,

$$\mathbb{P}(\mathbf{X}_{\mathcal{C}_m} = \mathbf{0}; G_{D0}) = (1 - p)^d. \quad (9)$$

Otherwise, when at least one AP has a packet to send, the channel will not idle. Because the Q_i s and T_i s are i.i.d. across nodes, and cliques are fully connected, each node in the clique has the same probability of occupying the channel. Thus, for any j , $j \in \{1, 2, \dots, |\mathcal{C}_m|\}$,

$$\mathbb{P}(\mathbf{X}_{\mathcal{C}_m} = \mathbf{e}_j; G_{D0}) = \frac{1 - (1 - p)^d}{d} \triangleq q, \quad (10)$$

Since the behavior of the cliques are independent, we have

$$P_0(\mathbf{x}) = \prod_{m=1}^{m_0+1} \mathbb{P}(\mathbf{X}_{\mathcal{C}_m} = \mathbf{x}_{\mathcal{C}_m}; G_{D0}). \quad (11)$$

2) Construct $M = n$ graphs: In this subsection, we construct a sequence of graphs $G_{D1}, G_{D2}, \dots, G_{DM}$. We construct n graphs, i.e., $M = n$. We construct each graph by picking a pair of nodes from distinct cliques in first m_0 cliques in graph G_{D0} . We add an edge between the selected pair. We leave the last $((m_0 + 1)$ th) clique unmodified for all G_{D1}, \dots, G_{DM} . We can construct $\binom{m_0}{2} d^2 = d^2 m_0(m_0 - 1)/2$ distinct graphs in this manner. Under the assumption that

$$d \leq n/2, \quad (12)$$

and the fact that $m_0 = \lfloor \frac{n}{d} \rfloor \geq \frac{n}{d} - 1$, we lower bound this number of graphs as

$$\begin{aligned} \frac{d^2}{2} m_0(m_0 - 1) &\geq \frac{d^2}{2} \left(\frac{n}{d} - 1 \right) \left(\frac{n}{d} - 2 \right) \\ &= d^2 - \frac{3n}{2}d + \frac{n^2}{2} \end{aligned} \quad (13)$$

This is a quadratic function of d for any fixed n . We want to construct $M = n$ graphs and the value of (13) equals n if

$$d = \frac{3n \pm \sqrt{n^2 + 16n}}{4}. \quad (14)$$

Since $d \leq n$, and $\sqrt{n^2 + 16n} > n$, only the smaller solution is feasible. When $n \geq 7$, we have $\frac{3n - \sqrt{n^2 + 16n}}{4} > 2$, thus the assumption $d \geq 2$ can be satisfied. Meanwhile, since

$$\frac{3n - \sqrt{n^2 + 16n}}{4} \leq \frac{3n - n}{4} = \frac{n}{2}, \quad (15)$$

the smaller solution of (14) is a tighter constraint on d than (12). Therefore, under the condition that

$$n \geq 7, \quad 2 \leq d \leq \frac{3n - \sqrt{n^2 + 16n}}{4},$$

we have $d^2 m_0(m_0 - 1)/2 \geq n$ and thus we can always pick n graphs that are perturbations of G_{D0} in the above sense. We note that for each of these graphs $D_L(G_{D0}, G_{Di}) = 1$, and $D_L(G_{Di}, G_{Dj}) = 2$ for any $0 < i, j \leq M$ where $i \neq j$.

3) G_{D1} and its transmission pattern distribution $P_1(\mathbf{x})$: We now calculate $P_1(\mathbf{x})$, which differs from $P_0(\mathbf{x})$ due to the added constraint resulting from the additional edge. Due to the symmetric construction of the M graphs, without loss of generality we concentrate on a single graph. Let G_{D1} be the graph formed from G_{D0} by connecting the i th node in \mathcal{C}_1 to the j th node in \mathcal{C}_2 with an edge. Since the remaining $m_0 - 2$ cliques are unchanged, the distribution of their transmission patterns $\mathbf{X}_{\mathcal{C}_m}$ is the same as under G_{D0} . Furthermore, the remaining transmission patterns are independent of each other and of $(\mathbf{X}_{\mathcal{C}_1}, \mathbf{X}_{\mathcal{C}_2})$. Thus we express the transmission pattern distribution under G_{D1} as

$$P_1(\mathbf{x}) = \mathbb{P}(\mathbf{X}_{\mathcal{C}_1} = \mathbf{x}_{\mathcal{C}_1}, \mathbf{X}_{\mathcal{C}_2} = \mathbf{x}_{\mathcal{C}_2}; G_{D1}) \cdot \prod_{m=3}^{m_0+1} \mathbb{P}(\mathbf{X}_{\mathcal{C}_m} = \mathbf{x}_{\mathcal{C}_m}; G_{D0}). \quad (16)$$

We want to calculate the KL-divergence between $P_0(\mathbf{x})$ from (11) and $P_1(\mathbf{x})$. The final $m_0 - 2$ terms of both are identical. Thus, for the remainder of this subsection we focus on the distribution of the activation pattern in the first two cliques, i.e., $\mathbb{P}(\mathbf{X}_{\mathcal{C}_1} = \mathbf{x}_{\mathcal{C}_1}, \mathbf{X}_{\mathcal{C}_2} = \mathbf{x}_{\mathcal{C}_2}; G_{D1})$.

The differences between $\mathbb{P}(\mathbf{X}_{\mathcal{C}_1} = \mathbf{x}_{\mathcal{C}_1}, \mathbf{X}_{\mathcal{C}_2} = \mathbf{x}_{\mathcal{C}_2}; G_{D1})$ and $\mathbb{P}(\mathbf{X}_{\mathcal{C}_1} = \mathbf{x}_{\mathcal{C}_1}, \mathbf{X}_{\mathcal{C}_2} = \mathbf{x}_{\mathcal{C}_2}; G_{D0})$ are due to the added edge, which constrains the allowable patterns. In particular, the event $\mathbf{X}_{\mathcal{C}_1} = \mathbf{e}_i, \mathbf{X}_{\mathcal{C}_2} = \mathbf{e}_j$, which occurs with nonzero probability under G_{D0} , cannot occur under G_{D1} . If, under G_{D0} both nodes i and j would have transmitted, under G_{D1} only one will transmit. The carrier sensing mechanism will suppress the transmission of the other. Which node will transmit and which will be suppressed depends on the respective

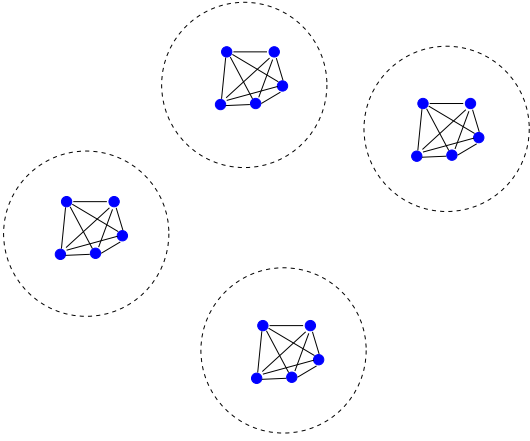


Fig. 6. A network consists of n/d cliques, where nodes in each clique are within each other's carrier sensing range. Nodes belonging to different cliques cannot hear each other. $n = 20, d = 5$.

back-off times. The result will be an increase in the probability of some other node transmitting, since the suppressed node will not compete for the channel.

To get the analysis rolling, we first consider the simpler situations of joint transmission patterns $(\mathbf{x}_{C_1}, \mathbf{x}_{C_2})$ where there is no possibility that transmission by node i could have suppressed transmission by node j (or vice-versa). For these situations the probability of the joint pattern under G_{D1} is the same as under G_{D0} . There are three such cases. The first case consists of patterns such that (i) some node in C_i other than i transmits and (ii) no node in C_2 transmits, i.e., $\mathbf{x}_{C_1} \in \mathcal{X}_1 \setminus \mathbf{e}_i$ and $\mathbf{x}_{C_2} = \mathbf{0}$. Condition (i) means that node i could not have suppressed the transmission of node j . Thus, by condition (ii) no node in C_2 has any data to transmit. Therefore,

$$\mathbb{P}(\mathbf{X}_{C_1} = \mathbf{x}_{C_1}, \mathbf{X}_{C_2} = \mathbf{0}; G_{D1}) = \mathbb{P}(\mathbf{X}_{C_1} = \mathbf{x}_{C_1}, \mathbf{X}_{C_2} = \mathbf{0}; G_{D0}).$$

The second case is the reverse of the first, i.e., (i) $\mathbf{x}_{C_2} \in \mathcal{X}_2 \setminus \mathbf{e}_j$ and (ii) $\mathbf{x}_{C_1} = \mathbf{0}$. By the same logic, $\mathbb{P}(\mathbf{X}_{C_1} = \mathbf{0}, \mathbf{X}_{C_2} = \mathbf{x}_{C_2}; G_{D1}) = \mathbb{P}(\mathbf{X}_{C_1} = \mathbf{0}, \mathbf{X}_{C_2} = \mathbf{x}_{C_2}; G_{D0})$. The third case consists of situations where (i) transmissions occur in both cliques, but (ii) neither i nor j transmit. Condition (ii) implies that suppression of node j by node i (or i by j) could not have occurred, and thus the probability of the joint pattern under G_{D1} is the same as under G_{D0} . These conditions are summarized as $\mathbf{x}_{C_1} \in \mathcal{X}_1 \setminus \{\mathbf{0}, \mathbf{e}_i\}$ and $\mathbf{x}_{C_2} \in \mathcal{X}_2 \setminus \{\mathbf{0}, \mathbf{e}_j\}$. Thus,

$$\mathbb{P}(\mathbf{X}_{C_1} = \mathbf{x}_{C_1}, \mathbf{X}_{C_2} = \mathbf{x}_{C_2}; G_{D1}) = \mathbb{P}(\mathbf{X}_{C_1} = \mathbf{x}_{C_1}, \mathbf{X}_{C_2} = \mathbf{x}_{C_2}; G_{D0}).$$

Finally, by (10) and (11) we know that $\mathbb{P}(\mathbf{X}_{C_1} = \mathbf{x}_{C_1}, \mathbf{X}_{C_2} = \mathbf{x}_{C_2}; G_{D0}) = q^2$.

We now turn to transmission patterns where nodes i and j interact. These are patterns $(\mathbf{x}_{C_1}, \mathbf{x}_{C_2})$ the probability of which may be higher under G_{D1} than under G_{D0} due to the infeasibility of the pattern $(\mathbf{e}_i, \mathbf{e}_j)$ under G_{D1} . To analyze these patterns consider the paired queue/backoff-time vectors $(\mathbf{Q}_{C_1 \cup C_2}, \mathbf{T}_{C_1 \cup C_2})$ that, under G_{D0} , would have resulted in $(\mathbf{X}_{C_1}, \mathbf{X}_{C_2}) = (\mathbf{e}_i, \mathbf{e}_j)$. Obviously, we must have $\mathbf{Q}_{C_1}, \mathbf{Q}_{C_2} \neq \mathbf{0}$. Depending on the particular realization of $(\mathbf{Q}_{C_1 \cup C_2}, \mathbf{T}_{C_1 \cup C_2})$ there are four possible outcomes under G_{D1} :

- (a) $T_i < T_j$ and $\mathbf{Q}_{C_2} = \mathbf{e}_j$: Node i will get the channel and transmit so $\mathbf{X}_{C_1} = \mathbf{e}_i$. However, the transmission of node j will be suppressed. Since $\mathbf{Q}_{C_2} = \mathbf{e}_j$, node j is the only node in C_2 with data, so $\mathbf{X}_{C_2} = \mathbf{0}$.
- (b) $T_i > T_j$ and $\mathbf{Q}_{C_1} = \mathbf{e}_i$: The analysis here is analogous to (a) with the roles of i and j reversed. Thus, the transmission pattern will be $\mathbf{X}_{C_1} = \mathbf{0}, \mathbf{X}_{C_2} = \mathbf{e}_j$.
- (c) $T_i < T_j$ and $\mathbf{Q}_{C_2} \neq \mathbf{e}_j$: In this situation at least one other node in C_2 has data to transmit. Thus, even though $\mathbf{X}_{C_1} = \mathbf{e}_i$ suppresses the transmission of node j , some other node in C_2 will transmit. Thus, $\mathbf{X}_{C_2} \in \mathcal{X}_2 \setminus \{\mathbf{e}_j, \mathbf{0}\}$. Furthermore, since the statistics of the queue statuses and backoff times are identical for all nodes, the transmitting node in C_2 will be uniformly distributed across the other $d - 2$ nodes in that clique.
- (d) $T_i > T_j$ and $\mathbf{Q}_{C_1} \neq \mathbf{e}_i$: The analysis here is analogous to (c) with the roles of i and j reversed. $\mathbf{X}_{C_2} = \mathbf{e}_j$, and \mathbf{X}_{C_1} is uniformly distributed across $\mathbf{x}_{C_1} \in \mathcal{X}_1 \setminus \{\mathbf{e}_i, \mathbf{0}\}$.

We note that the above four cases partition the event space where nodes i and j transmit concurrently under G_{D0} . The four terms in the following correspond, respectively, to (a)–(d), above:

$$\begin{aligned} & \mathbb{P}(\mathbf{X}_{C_1} = \mathbf{e}_i, \mathbf{X}_{C_2} = \mathbf{e}_j; G_{D0}) \\ &= \mathbb{P}(\mathbf{X}_{C_1} = \mathbf{e}_i, \mathbf{X}_{C_2} = \mathbf{e}_j, T_i < T_j, \mathbf{Q}_{C_2} = \mathbf{e}_j; G_{D0}) \\ & \quad + \mathbb{P}(\mathbf{X}_{C_1} = \mathbf{e}_i, \mathbf{X}_{C_2} = \mathbf{e}_j, T_i > T_j, \mathbf{Q}_{C_1} = \mathbf{e}_i; G_{D0}) \\ & \quad + \mathbb{P}(\mathbf{X}_{C_1} = \mathbf{e}_i, \mathbf{X}_{C_2} = \mathbf{e}_j, T_i < T_j, \mathbf{Q}_{C_2} \neq \mathbf{e}_j; G_{D0}) \\ & \quad + \mathbb{P}(\mathbf{X}_{C_1} = \mathbf{e}_i, \mathbf{X}_{C_2} = \mathbf{e}_j, T_i > T_j, \mathbf{Q}_{C_1} \neq \mathbf{e}_i; G_{D0}) \\ &= 2\beta_1 + 2\beta_2. \end{aligned} \tag{17}$$

The first two terms are equal due to the symmetry of the conditions and graph structure. Similar logic implies that the third and fourth terms are also equal. We respectively define β_1 and β_2 to be the two probabilities.

We now consider the four cases of joint transmission patterns $(\mathbf{x}_{C_1}, \mathbf{x}_{C_2})$ under G_{D1} not yet considered. These will each connect to one of the cases (a)–(d), above. First, consider the probability of pattern $(\mathbf{x}_{C_1}, \mathbf{x}_{C_2}) = (\mathbf{e}_i, \mathbf{0})$ under G_{D1} . The probability of this pattern under G_{D1} will be larger than under G_{D0} since certain pairs (\mathbf{Q}, \mathbf{T}) that result in $(\mathbf{e}_i, \mathbf{e}_j)$ under G_{D0} result in $(\mathbf{e}_i, \mathbf{0})$ under G_{D1} . The probability of observing $(\mathbf{e}_i, \mathbf{0})$ under G_{D1} equals the probability of observing that pattern under G_{D0} plus the probability of the event occurring that was considered in case (a), above. This latter event is the bump in probability due to the interaction of i and j . Therefore, we find that

$$\begin{aligned} & \mathbb{P}(\mathbf{X}_{C_1} = \mathbf{e}_i, \mathbf{X}_{C_2} = \mathbf{0}; G_{D1}) \\ &= \mathbb{P}(\mathbf{X}_{C_1} = \mathbf{e}_i, \mathbf{X}_{C_2} = \mathbf{0}; G_{D0}) \\ & \quad + \mathbb{P}(\mathbf{X}_{C_1} = \mathbf{e}_i, \mathbf{X}_{C_2} = \mathbf{e}_j, T_i < T_j, \mathbf{Q}_{C_2} = \mathbf{e}_j; G_{D0}) \\ &= q(1 - p)^d + \beta_1, \end{aligned} \tag{18}$$

where the first term follows from the independence of the node-wise transmission patterns under G_{D0} , from the definition of the probability q in (10), and from the fact that with probability $(1 - p)^d$ no nodes in C_2 have data to transmit. We defer the calculation of $\beta_1 = \mathbb{P}(\mathbf{X}_{C_1} = \mathbf{e}_i, \mathbf{X}_{C_2} = \mathbf{e}_j, T_i <$

$T_j, \mathbf{Q}_{C_2} = \mathbf{e}_j; G_{D0}$) until (23). Following a similar line of argument for $(\mathbf{x}_{C_1}, \mathbf{x}_{C_2}) = (\mathbf{0}, \mathbf{e}_j)$, and considering case (b), we find that

$$\mathbb{P}(\mathbf{X}_{C_1} = \mathbf{0}, \mathbf{X}_{C_2} = \mathbf{e}_j; G_{D1}) = q(1-p)^d + \beta_1. \quad (19)$$

The third case concerns the patterns $(\mathbf{e}_i, \mathbf{x}_{C_2})$ for all $\mathbf{x}_{C_2} \in \mathcal{X}_2 \setminus \{\mathbf{0}, \mathbf{e}_j\}$. Similar to (a) and (b), the probability of a pattern in this set will be at least as large as the probability of the pattern under G_{D0} due to a boost in probability resulting from the infeasibility of the $(\mathbf{e}_i, \mathbf{e}_j)$ pattern under G_{D1} . The boost corresponds to the event discussed in (c), above. For any $\mathbf{x}_{C_2} \in \mathcal{X}_2 \setminus \{\mathbf{e}_j, \mathbf{0}\}$ we find that

$$\begin{aligned} & \mathbb{P}(\mathbf{X}_{C_1} = \mathbf{e}_i, \mathbf{X}_{C_2} = \mathbf{x}_{C_2}; G_{D1}) \\ &= \mathbb{P}(\mathbf{X}_{C_1} = \mathbf{e}_i, \mathbf{X}_{C_2} = \mathbf{x}_{C_2}; G_{D0}) \\ &+ \frac{1}{d-2} \mathbb{P}(\mathbf{X}_{C_1} = \mathbf{e}_i, \mathbf{X}_{C_2} = \mathbf{e}_j, T_i < T_j, \mathbf{Q}_{C_2} \neq \mathbf{e}_j; G_{D0}) \\ &= q^2 + \frac{1}{d-1} \beta_2. \end{aligned} \quad (20)$$

The factor of $1/(d-1)$ in the second term results from the uniformity over the other $d-1$ transmission patterns in \mathcal{C}_2 , mentioned in (c). The probability $\beta_2 = \mathbb{P}(\mathbf{X}_{C_1} = \mathbf{e}_i, \mathbf{X}_{C_2} = \mathbf{e}_j, T_i < T_j, \mathbf{Q}_{C_2} \neq \mathbf{e}_j; G_{D0})$ will be calculated in (24). Finally, by symmetric logic, we find that for any $\mathbf{x}_{C_1} \in \mathcal{X}_1 \setminus \{\mathbf{e}_i, \mathbf{0}\}$

$$\mathbb{P}(\mathbf{X}_{C_1} = \mathbf{x}_{C_1}, \mathbf{X}_{C_2} = \mathbf{e}_j; G_{D1}) = q^2 + \frac{1}{d-1} \beta_2. \quad (21)$$

We now calculate β_1 , required in (18) and (19). We start by rewriting the first term (17) using Bayes' rule as

$$\begin{aligned} & \mathbb{P}(\mathbf{X}_{C_1} = \mathbf{e}_i, \mathbf{X}_{C_2} = \mathbf{e}_j, T_i < T_j, \mathbf{Q}_{C_2} = \mathbf{e}_j; G_{D0}) \\ &= \mathbb{P}(\mathbf{X}_{C_1} = \mathbf{e}_i, T_i < T_j; G_{D0}) \mathbb{P}(\mathbf{X}_{C_2} = \mathbf{e}_j, \mathbf{Q}_{C_2} = \mathbf{e}_j; G_{D0}). \end{aligned}$$

In the application of Bayes' rule we have used the fact that $\mathbb{P}(\mathbf{X}_{C_1} = \mathbf{e}_i, T_i < T_j | \mathbf{X}_{C_2} = \mathbf{e}_j, \mathbf{Q}_{C_2} = \mathbf{e}_j; G_{D0}) = \mathbb{P}(\mathbf{X}_{C_1} = \mathbf{e}_i, T_i < T_j; G_{D0})$, due to the independence of transmission patterns under G_{D0} . Now, note that $\mathbb{P}(\mathbf{X}_{C_2} = \mathbf{e}_j, \mathbf{Q}_{C_2} = \mathbf{e}_j; G_{D0}) = p(1-p)^{d-1}$ as node j is the only node in \mathcal{C}_2 with something to transmit. Define $\mathcal{T}_{1,i} = \{j \in \mathcal{C}_1 : T_j < T_i\}$, i.e., the set of APs in \mathcal{C}_1 whose backoff time is shorter than that of AP i . Next, rewrite $\mathbb{P}(\mathbf{X}_{C_1} = \mathbf{e}_i, T_i < T_j; G_{D0})$ as

$$\begin{aligned} & \sum_{l=0}^{d-1} \mathbb{P}(\mathbf{X}_{C_1} = \mathbf{e}_i, T_i < T_j, |\mathcal{T}_{1,i}| = l; G_{D0}) \\ &= \sum_{l=0}^{d-1} \mathbb{P}(\mathbf{X}_{C_1} = \mathbf{e}_i | T_i < T_j, |\mathcal{T}_{1,i}| = l; G_{D0}) \\ &\quad \cdot \mathbb{P}(T_i < T_j, |\mathcal{T}_{1,i}| = l; G_{D0}). \end{aligned}$$

The first factor $\mathbb{P}(\mathbf{X}_{C_1} = \mathbf{e}_i | T_i < T_j, |\mathcal{T}_{1,i}| = l; G_{D0}) = p(1-p)^l$. The second factor is just the fraction of the $d!$ orderings such that there are l nodes in \mathcal{C}_1 with backoff times lower than T_i and such that node $T_i < T_j$. The number of such orderings is $\binom{d-1}{l} l!(d-l)! = (d-1)!(d-l)$. Putting the

pieces together we find that

$$\begin{aligned} \beta_1 &\triangleq \mathbb{P}(\mathbf{X}_{C_1} = \mathbf{e}_i, \mathbf{X}_{C_2} = \mathbf{e}_j, T_i < T_j, \mathbf{Q}_{C_2} = \mathbf{e}_j; G_{D0}) \\ &= \mathbb{P}(\mathbf{X}_{C_1} = \mathbf{e}_i, T_i < T_j; G_{D0}) \mathbb{P}(\mathbf{X}_{C_2} = \mathbf{e}_j, \mathbf{Q}_{C_2} = \mathbf{e}_j; G_{D0}) \\ &= \left[\sum_{l=0}^{d-1} (d-l)(1-p)^l \right] \frac{p^2(1-p)^{(d-1)}}{d(d+1)} \\ &= \frac{(p(d+1) - 1 + (1-p)^{d+1})(1-p)^{(d-1)}}{d(d+1)}. \end{aligned} \quad (22)$$

And, since transmitters i and j have the same statistics, when $T_i > T_j$, we also have

$$\mathbb{P}(\mathbf{X}_{C_1} = \mathbf{e}_i, \mathbf{X}_{C_2} = \mathbf{e}_j, T_i > T_j, \mathbf{Q}_{C_1} = \mathbf{e}_i; G_{D0}) = \beta_1,$$

which justifies (19).

Finally, to calculate β_2 we simply combine (17) with (23).

$$\mathbb{P}(\mathbf{X}_{C_1} = \mathbf{e}_i, \mathbf{X}_{C_2} = \mathbf{e}_j; G_{D0}) = 2\beta_1 + 2\beta_2 = q^2,$$

where the final inequality follows from the independence of \mathbf{X}_{C_1} and \mathbf{X}_{C_2} under G_{D0} . Thus,

$$\beta_2 = \frac{q^2 - 2\beta_1}{2}. \quad (24)$$

4) *Bounding $D_{KL}(P_0 \| P_1)$* : The Kullback-Leibler divergence between the distribution of transmission patterns under G_{D1} and G_{D0} , denoted as P_1 and P_0 , respectively, can be calculated as

$$\begin{aligned} D_{KL}(P_1 \| P_0) &= \sum_{\mathbf{x} \in \{0,1\}^n} P_1(\mathbf{x}) \log \frac{P_1(\mathbf{x})}{P_0(\mathbf{x})} \\ &= \sum_{\mathbf{x}_{C_1} \in \{0,1\}^d, \mathbf{x}_{C_2} \in \{0,1\}^d} \mathbb{P}(\mathbf{X}_{C_1} = \mathbf{x}_{C_1}, \mathbf{X}_{C_2} = \mathbf{x}_{C_2}; G_{D1}) \\ &\quad \cdot \log \frac{\mathbb{P}(\mathbf{X}_{C_1} = \mathbf{x}_{C_1}, \mathbf{X}_{C_2} = \mathbf{x}_{C_2}; G_{D1})}{\mathbb{P}(\mathbf{X}_{C_1} = \mathbf{x}_{C_1}; G_{D0}) \mathbb{P}(\mathbf{X}_{C_2} = \mathbf{x}_{C_2}; G_{D0})} \end{aligned} \quad (25)$$

$$\begin{aligned} &= 2\mathbb{P}(\mathbf{X}_{C_1} = \mathbf{e}_i, \mathbf{X}_{C_2} = \mathbf{0}; G_{D1}) \\ &\quad \cdot \log \frac{\mathbb{P}(\mathbf{X}_{C_1} = \mathbf{e}_i, \mathbf{X}_{C_2} = \mathbf{0}; G_{D1})}{\mathbb{P}(\mathbf{X}_{C_1} = \mathbf{e}_i; G_{D0}) \mathbb{P}(\mathbf{X}_{C_2} = \mathbf{0}; G_{D0})} \\ &+ 2(d-1) \mathbb{P}(\mathbf{X}_{C_1} = \mathbf{e}_i, \mathbf{X}_{C_2} = \mathbf{e}_{j'}; G_{D1}) \\ &\quad \cdot \log \frac{\mathbb{P}(\mathbf{X}_{C_1} = \mathbf{e}_i, \mathbf{X}_{C_2} = \mathbf{e}_{j'}; G_{D1})}{\mathbb{P}(\mathbf{X}_{C_1} = \mathbf{e}_i; G_{D0}) \mathbb{P}(\mathbf{X}_{C_2} = \mathbf{e}_{j'}; G_{D0})} \end{aligned} \quad (26)$$

$$\begin{aligned} &= 2[q(1-p)^d + \beta_1] \log \left[\frac{q(1-p)^d + \beta_1}{q(1-p)^d} \right] \\ &+ 2(d-1) \left[q^2 + \frac{\beta_2}{d-1} \right] \log \left[\frac{q^2 + \frac{\beta_2}{d-1}}{q^2} \right] \end{aligned} \quad (27)$$

$$\leq \frac{2\beta_1}{q(1-p)^d} (q(1-p)^d + \beta_1) + \frac{2\beta_2}{q^2} \left(q^2 + \frac{\beta_2}{d-1} \right) \quad (28)$$

$$= q^2 + \frac{2\beta_1^2}{q(1-p)^d} + \frac{2\beta_2^2}{(d-1)q^2}. \quad (29)$$

In (25) we cancel (and marginalize over) the $m_0 - 1$ common factors of the form $\mathbb{P}(\mathbf{X}_{C_m} = \mathbf{x}_{C_m}; G_{D0})$, $3 \leq m \leq m_0 + 1$ cf. (11) and (16). In (26), we focus on the terms that don't cancel out. The first two terms therein correspond to cases (a) and (b), cf. (18) and (19). The latter $2(d-2)$ terms correspond to the cases (c) and (d), cf. (20) and (21), where j' is some node $j' \in \mathcal{C}_2$ but $j' \neq j$. In (27) we use (18) and (20) in

the numerators and (9) and (11) in the denominators. The inequality in (28) follows from the fact that $\log(1+x) \leq x$. Based on the definitions of q , β_1 and β_2 from (10), (23) and (24), we have

$$\begin{aligned} \frac{2\beta_1^2}{q(1-p)^d} &= \frac{2\beta_1}{q} \frac{\beta_1}{(1-p)^d} \\ &= \frac{2\beta_1}{1-(1-p)^d} \frac{1}{d+1} \left(\frac{dp}{1-p} - 1 + (1-p)^d \right) \\ &\leq \frac{2\beta_1}{d+1} \left(\frac{d}{1-(1-p)^d} \cdot \frac{p}{1-p} - 1 \right) \leq \frac{2\beta_1}{1-p} \end{aligned} \quad (30)$$

and

$$\frac{2\beta_2^2}{(d-1)q^2} = \frac{\beta_2}{d-1} \frac{2\beta_2}{q^2} \leq \beta_2 \leq q^2. \quad (31)$$

Plugging (30) and (31) into (29), we have

$$D_{KL}(P_1 \| P_0) \leq \left(2 + \frac{1}{1-p} \right) \frac{1}{d^2}. \quad (32)$$

5) *Put pieces together:* Since the G_{Di} s are constructed in the same manner, $D_{KL}(P_i \| P_0) = D_{KL}(P_1 \| P_0)$ for all i . Thus, we have

$$\frac{1}{M} \sum_{i=1}^M D_{KL}(P_i \| P_0) \leq \left(2 + \frac{1}{1-p} \right) \frac{1}{d^2}.$$

In summary, we have $D_L(G_{Di}, G_{Dj}) \geq 1$ for $0 \leq i < j \leq M$ and we can always pick $M = n$. Thus, according to Thm. 5, when

$$k \leq \frac{\alpha \log n}{\left(2 + \frac{1}{1-p} \right) \frac{1}{d^2}}$$

we have

$$\begin{aligned} &\inf_{\hat{G}_D \in \mathcal{G}_d} \sup_{G_D \in \mathcal{G}_d} \mathbb{P}(\hat{G}_D \neq G_D; G_D) \\ &= \inf_{\hat{G}_D \in \mathcal{G}_d} \sup_{G_D \in \mathcal{G}_d} \mathbb{P}(D_L(\hat{G}_D, G_D) \geq 1/2; G_D) \\ &> \frac{\sqrt{n}}{1 + \sqrt{n}} \left(1 - 2\alpha - \sqrt{\frac{2\alpha}{\log n}} \right) > 0. \end{aligned}$$

C. Proof of Theorem 3

Before we prove Theorem 3, we first show that the following lemma is true.

Lemma 1 $\lim_{k \rightarrow \infty} \mathbb{P}(\hat{\mathcal{S}}_j(k) = \mathcal{S}_j) = 1$.

The lemma states that when k is sufficiently large, identifying the minimum hitting set of the candidate interferer sets is equivalent to identifying the hidden interferer set of an AP.

Proof: Since $Y_j = 0$ must be caused by some active interferer, $\mathcal{S}_j^t \cap \mathcal{S}_j \neq \emptyset$ for every $t \in \mathcal{K}_j(k)$. Therefore, \mathcal{S}_j is a hitting set for $\{\mathcal{S}_j^t\}_{t \in \mathcal{K}_j(k)}$.

Next, we prove that \mathcal{S}_j is the unique minimum hitting set. We prove this through contradiction. Assume that there exist a different hitting set $\hat{\mathcal{S}}_j(k)$ with $|\hat{\mathcal{S}}_j(k)| \leq |\mathcal{S}_j|$. Since $\hat{\mathcal{S}}_j(k)$ is different from \mathcal{S}_j , there must exist a node $i \in \mathcal{S}_j$, that is not in

$\hat{\mathcal{S}}_j(k)$, i.e., $i \in \mathcal{S}_j \setminus \hat{\mathcal{S}}_j(k)$. Consider the following probability

$$\begin{aligned} &\mathbb{P}(X_i = 1, X_j = 1, Y_j = 0, \mathbf{X}_{\hat{\mathcal{S}}_j(k)} = \mathbf{0}) \\ &= \mathbb{P}(X_i = 1, X_j = 1, \mathbf{X}_{\hat{\mathcal{S}}_j(k)} = \mathbf{0}) \\ &\quad \cdot \mathbb{P}(Y_j = 0 | X_i = 1, X_j = 1, \mathbf{X}_{\hat{\mathcal{S}}_j(k)} = \mathbf{0}) \\ &\geq \mathbb{P}(X_i = 1, X_j = 1, \mathbf{Q}_{\hat{\mathcal{S}}_j(k)} = \mathbf{0}) \\ &\quad \cdot \mathbb{P}(Y_j = 0 | X_i = 1, X_j = 1, \mathbf{X}_{\hat{\mathcal{S}}_j(k)} = \mathbf{0}) \\ &= \mathbb{P}(X_i = 1, X_j = 1 | \mathbf{Q}_{\hat{\mathcal{S}}_j(k)} = \mathbf{0}) \cdot \mathbb{P}(\mathbf{Q}_{\hat{\mathcal{S}}_j(k)} = \mathbf{0}) \\ &\quad \cdot \mathbb{P}(Y_j = 0 | X_i = 1, X_j = 1, \mathbf{X}_{\hat{\mathcal{S}}_j(k)} = \mathbf{0}) \\ &\geq \frac{p^2}{(d+1)^2} (1-p)^{|\hat{\mathcal{S}}_j(k)|} p_{ij} \geq \frac{p^2}{(d+1)^2} (1-p)^s p_{\min}, \end{aligned} \quad (33)$$

where the first inequality in (33) is based on the observation that given $\mathbf{Q}_{\hat{\mathcal{S}}_j(k)}$, the network behaves as if the APs in $\hat{\mathcal{S}}_j(k)$ do not exist at all. With fewer nodes and possibly fewer edges in the corresponding direct interference graph, the bound we derive in (8) is still valid. The second inequality in (33) follows from the assumptions that $i \in \mathcal{S}_j$, $|\hat{\mathcal{S}}_j(k)| \leq |\mathcal{S}_j| \leq s$, and from (2).

For any observation with $X_i(t) = 1, X_j(t) = 1, Y_j(t) = 0, \mathbf{X}_{\hat{\mathcal{S}}_j(k)}(t) = \mathbf{0}$, the time index t is an index of $\mathcal{K}_j(k)$. However, $\mathcal{S}_j^t \cap \hat{\mathcal{S}}_j(k) = \emptyset$. This contradicts the assumption that $\hat{\mathcal{S}}_j(k)$ is a hitting set. Since the probability of this event has a lower bound for any fixed d and s , this event happens with probability one as $k \rightarrow \infty$. Therefore, \mathcal{S}_j is the unique minimum hitting set as $k \rightarrow \infty$. ■

Define the error event E_j as the event that the estimated minimum hitting set $\hat{\mathcal{S}}_j(k)$ is not equal to \mathcal{S}_j after k observations. This only happens when $|\hat{\mathcal{S}}_j(k)| \leq |\mathcal{S}_j|$. So when $|\hat{\mathcal{S}}_j(k)| \leq |\mathcal{S}_j|$, there must exist at least one transmitter $i \in \mathcal{S}_j$ that is not included in $\hat{\mathcal{S}}_j(k)$. Then, following steps similar to those followed in the proof of Lemma 1, we have

$$\begin{aligned} \mathbb{P}(E_j) &= \mathbb{P}(\cup_{i \in \mathcal{S}_j} i \notin \hat{\mathcal{S}}_j(k)) \\ &\leq \sum_{i \in \mathcal{S}_j} (1 - \mathbb{P}(X_i = 1, X_j = 1, Y_j = 0, \mathbf{X}_{\hat{\mathcal{S}}_j(k)} = \mathbf{0}))^k \\ &\leq s \left(1 - \frac{p^2}{(d+1)^2} (1-p)^s p_{\min} \right)^k. \end{aligned}$$

Therefore,

$$\begin{aligned} \mathbb{P}(\hat{G}_H \neq G_H) &= \mathbb{P}(\cup_j E_j) \leq \sum_j s \left(1 - \frac{p^2}{d^2} (1-p)^{s-1} p_{\min} \right)^k \\ &= ns \left(1 - \frac{p^2(1-p)^s p_{\min}}{(d+1)^2} \right)^k. \end{aligned}$$

D. Proof of Theorem 4

To prove Theorem 4 we follow a similar approach to that taken in the proof of Theorem 2. For any given direct interference graph $G_D = (\mathcal{V}, \mathcal{E}_D)$, we define $\mathcal{H}_s(G_D)$ to be the set of hidden interference graphs satisfying the assumption that $s_j \leq s$ for every j . We construct a collections of graphs, $G_{H0}, G_{H1}, \dots, G_{HM}$, all in $\mathcal{H}_s(G_D)$, and reduce the interference graph estimation problem to an M -ary hypothesis test. These graphs share the same node set and direct inter-

ference edges, however, the hidden interference edges differ. With slight abuse of the notation, we use $P_i(\mathbf{x}, \mathbf{y})$ to denote the joint distribution of transmission pattern \mathbf{x} and feedback information vector \mathbf{y} under G_D and G_{Hi} , $0 \leq i \leq M$. We use $\mathbb{P}(\mathcal{A}; G_{Hi})$ to denote the probability of event \mathcal{A} under distribution $P_i(\mathbf{x}, \mathbf{y})$. Note that $\mathbb{P}(\mathcal{A}; G_{Hi})$ implicitly depends on the underlying direct interference graph G_D .

1) *Construct G_D and G_{H0}* : Assume $s \geq 2$. We now construct an underlying direct interference graph G_D , and add directed edges to form G_{H0} . An illustrative example of a possible G_D is provided in Fig. 7. We partition the node set into $\lceil n/(2(d+1) + s - 1) \rceil$ groups. The first $\lfloor n/(2(d+1) + s - 1) \rfloor$ groups consist of $2d + s - 1$ nodes. The last group consists of the remaining nodes. In each group, except the last, we cluster $2(d+1)$ nodes into a pair of cliques, each clique consisting of $d + 1$ nodes. The remaining $s - 1$ nodes are ‘‘independent’’ nodes or ‘‘atoms’’, disconnected from all other nodes in the network. Thus, their activation statuses depend only on their own queue statuses; they are independent of everything else.

We construct G_{H0} by adding directed edges to G_D . These edges will be added only between nodes in the same group. Hidden interference will thus exist only among nodes within the same group. It will not exist between groups. To construct the hidden interference G_{H0} consider each node in each clique in each group. Let all $s - 1$ independent nodes in that same group be hidden interferers as well as one (any one) node in the other clique in the same group. Thus every node in each clique has exactly s hidden interferers. We note that a node in a clique is allowed to interfere with more than one node in the other clique. The last group can have an arbitrary edge structure as long as it satisfies the maximum degree constraints.

Part of the hidden graph structure are the probabilities p_{ij} , defined in (1). Recall that p_{ij} tells us the likelihood that hidden interferer $i \in \mathcal{S}_j$ interferes with the transmission of node j . We now specify these probabilities for G_{H0} . For all $i \in \mathcal{S}_j$ and $\mathcal{S} \subseteq \mathcal{V} \setminus \{i, j\}$, the hidden interferers satisfy

$$\begin{aligned} \mathbb{P}(Y_j = 0 | X_i = 1, X_j = 1, \mathbf{X}_{\mathcal{V} \setminus \{i, j\}} = \mathbf{0}; G_{H0}) \\ = \mathbb{P}(Y_j = 0 | X_i = 1, X_j = 1, \mathbf{X}_{\mathcal{S}} = \mathbf{x}_{\mathcal{S}}; G_{H0}) = p_{\min}, \end{aligned} \quad (34)$$

where $\mathbf{x}_{\mathcal{S}}$ is any transmission pattern feasible under the direct interference graph G_D . Thus, in contrast to the inequality (2) in the general setting, for this network the bound holds with *equality* for all $i \in \mathcal{S}_j$. The implication is that the transmission collision probability for an AP j doesn’t increase if there is more than one hidden interferer transmitting. This assumption holds for every hidden interference graph G_{Hi} discussed in this section.

2) *Construct M hidden interference graphs*: We now construct a set of hidden interference graphs $G_{H1}, G_{H2}, \dots, G_{HM}$ as perturbations of G_{H0} . We construct each graph by removing a single directed edge in G_{H0} . The edge we remove connects a pair of nodes that are in distinct cliques in a single group in G_{H0} . To get the graph we do not remove an edge between an independent node and a node in a clique.

In each group, there are $2(d+1)$ such edges. There are thus

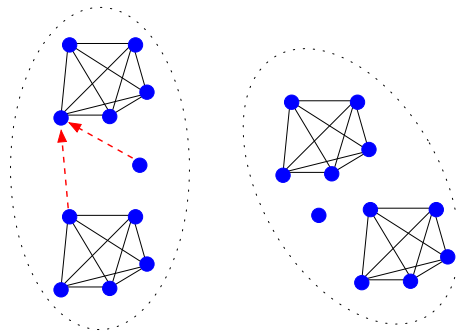


Fig. 7. A direct interference graph G_D of $n/(2(d+1) + s - 1) = 2$ groups, where each group consists of two fully connected cliques of size $d + 1$ and $s - 1$ detached APs; Dashed arrows indicate the hidden interferers of one node; $n = 22, d = 4, s = 2$.

$2(d+1)\lfloor n/(2(d+1) + s - 1) \rfloor$ distinct edges in G_{H0} that can be removed. If

$$d + 1 \leq c_1 n, \quad s - 1 \leq c_2 n, \quad \text{and} \quad 2c_1 + c_2 < 1, \quad (35)$$

where c_1, c_2 are positive constants, then there are more than $2c_1(\frac{1}{2c_1+c_2} - 1)n := M$ such edges. For each of these graphs, $D_L(D_{H0}, D_{Hi}) = 1$ and $D_L(D_{Hi}, D_{Hj}) = 2$ where $1 \leq i, j \leq M$.

3) *Characterize $D_{KL}(P_1 || P_0)$* : Without loss of generality, we assume that one directed edge (i, j) is removed from G_{H0} to form G_{H1} , where $i \in \mathcal{C}_1$, and $j \in \mathcal{C}_2$. Since we are removing an edge from G_{H0} to get G_{H1} , the probability defined in (34) is inherited. Thus, the only difference between the distributions under G_{H1} and G_{H0} occurs when $\mathbf{X}_{\mathcal{C}_1} = \mathbf{e}_i$, $\mathbf{X}_{\mathcal{C}_2} = \mathbf{e}_j$, and $\mathbf{X}_{\mathcal{S}_j \setminus i} = \mathbf{0}$. Specifically,

$$\mathbb{P}(Y_j = 0 | \mathbf{X}_{\mathcal{C}_1} = \mathbf{e}_i, \mathbf{X}_{\mathcal{C}_2} = \mathbf{e}_j, \mathbf{X}_{\mathcal{S}_j \setminus i} = \mathbf{0}; G_{H0}) = p_{\min},$$

while

$$\mathbb{P}(Y_j = 0 | \mathbf{X}_{\mathcal{C}_1} = \mathbf{e}_i, \mathbf{X}_{\mathcal{C}_2} = \mathbf{e}_j, \mathbf{X}_{\mathcal{S}_j \setminus i} = \mathbf{0}; G_{H1}) = 0.$$

Therefore,

$$\begin{aligned} D_{KL}(P_1 || P_0) &= \sum_{\mathbf{x}, \mathbf{y}} P_1(\mathbf{x}, \mathbf{y}) \log \frac{P_1(\mathbf{x}, \mathbf{y})}{P_0(\mathbf{x}, \mathbf{y})} \\ &= \sum_{\mathbf{x}, \mathbf{y}} P_1(\mathbf{x}) P_1(\mathbf{y} | \mathbf{x}) \log \frac{P_1(\mathbf{y} | \mathbf{x}) P_1(\mathbf{x})}{P_0(\mathbf{y} | \mathbf{x}) P_0(\mathbf{x})} \\ &= \mathbb{P}(\mathcal{A}; G_{H1}) \sum_{y_j \in \{0, 1\}} P_1(y_j | \mathcal{A}) \log \frac{P_1(y_j | \mathcal{A})}{P_0(y_j | \mathcal{A})} \\ &= - \left(\frac{1 - (1 - p)^{d+1}}{d + 1} \right)^2 (1 - p)^{s-1} \log(1 - p_{\min}) \end{aligned}$$

where $P_1(\mathbf{x}) = P_0(\mathbf{x})$ since G_D is held fixed, $\mathcal{A} := \{\mathbf{X}_{\mathcal{C}_1} = \mathbf{e}_i, \mathbf{X}_{\mathcal{C}_2} = \mathbf{e}_j, \mathbf{X}_{\mathcal{S}_j \setminus i} = \mathbf{0}\}$. $\mathbb{P}(\mathcal{A}; G_{H1}) = \mathbb{P}(\mathbf{X}_{\mathcal{C}_1} = \mathbf{e}_i; G_{H1}) \mathbb{P}(\mathbf{X}_{\mathcal{C}_2} = \mathbf{e}_j; G_{H1}) \mathbb{P}(\mathbf{X}_{\mathcal{S}_j \setminus i} = \mathbf{0}; G_{H1})$ because \mathcal{C}_1 , \mathcal{C}_2 and $\mathcal{S}_j \setminus i$ are disconnected in G_D . $\mathbb{P}(\mathcal{A}; G_{H1})$ is then calculated following a similar sequence of steps as used to obtain (11).

4) *Put the pieces together*: In summary, we have $M = 2c_1(\frac{1}{2c_1+c_2} - 1)n$ and $D_L(G_{Hi}, G_{Hj}) \geq 1$ for $0 \leq i < j \leq M$. Theorem 4 is proved by an application of Theorem 5.

REFERENCES

- [1] J. Yang, S. Draper, and R. Nowak, "Passive learning of the interference graph of a wireless network," *IEEE International Symposium on Information Theory*, pp. 2735–2740, July 2012.
- [2] D. Niculescu, "Interference map for 802.11 networks," in *Proceedings of the 7th ACM SIGCOMM Conference on Internet Measurement, 2007*, pp. 339–350.
- [3] N. Ahmed and S. Keshav, "Smarta: A self-managing architecture for thin access points," in *Proceedings of the 2006 ACM CoNEXT Conference, 2006*, pp. 9:1–9:12.
- [4] B. N. L. Liu, Y. Li and Z. Pi, "Heterogeneous cellular networks," in *Radio Resource and Interference Management for Heterogeneous Networks*, R. Q. Hu and Y. Qian, Eds. Jon Wiley & Sons, 2013, ch. 2.
- [5] V. V. Shrivastava, "Optimizing enterprise wireless networks through centralization," Ph.D. dissertation, University of Wisconsin–Madison, 2010.
- [6] V. Shrivastava, S. Rayanchu, S. Banerjee, and K. Papagiannaki, "PIE in the sky: Online passive interference estimation for enterprise WLANs," in *Proceedings of the 8th USENIX Conference on Networked Systems Design and Implementation, 2011*, pp. 337–350.
- [7] Y.-C. Cheng, J. Bellardo, P. Benkő, A. C. Snoeren, G. M. Voelker, and S. Savage, "Jigsaw: Solving the puzzle of enterprise 802.11 analysis," *ACM SIGCOMM*, vol. 36, no. 4, pp. 39–50, Aug. 2006.
- [8] Y.-C. Cheng, M. Afanasyev, P. Verkaik, P. Benkő, J. Chiang, A. C. Snoeren, S. Savage, and G. M. Voelker, "Automating cross-layer diagnosis of enterprise wireless networks," *ACM SIGCOMM*, vol. 37, no. 4, pp. 25–36, Aug. 2007.
- [9] R. Mahajan, M. Rodrig, D. Wetherall, and J. Zahorjan, "Analyzing the MAC-level behavior of wireless networks in the wild," *ACM SIGCOMM*, vol. 36, no. 4, pp. 75–86, Aug. 2006.
- [10] R. Castro, M. Coates, G. Liang, R. Nowak, and B. Yu, "Network tomography: Recent developments," *Statistical Science*, vol. 19, pp. 499–517, 2004.
- [11] N. G. Duffield, J. Horowitz, F. L. Presti, and D. F. Towsley, "Multicast topology inference from measured end-to-end loss," *IEEE Transactions on Information Theory*, vol. 48, no. 1, pp. 26–45, 2002.
- [12] R. Castro, M. Coates, and R. Nowak, "Likelihood based hierarchical clustering," *IEEE Transactions on Signal Processing*, vol. 52, no. 8, pp. 2308–2321, Aug. 2004.
- [13] P. Sattari, C. Fragouli, and A. Markopoulou, "Active topology inference using network coding," *Physical Communication*, vol. 6, pp. 142–163, 2013.
- [14] G. Atia and V. Saligrama, "Boolean compressed sensing and noisy group testing," *IEEE Transactions on Information Theory*, vol. 58, no. 3, pp. 1880–1901, 2012.
- [15] M. Cheraghchi, A. Karbasi, S. Mohajer, and V. Saligrama, "Graph-constrained group testing," *IEEE Transactions on Information Theory*, vol. 58, no. 1, pp. 248–262, Jan. 2012.
- [16] T. Tošić, N. Thomos, and P. Frossard, "Distributed sensor failure detection in sensor networks," *Signal Processing*, vol. 93, no. 2, pp. 399–410, Feb. 2013.
- [17] Y. Lin, W. Bao, W. Yu, and B. Liang, "Optimizing user association and spectrum allocation in HetNets: A utility perspective," *IEEE Journal on Selected Areas in Communications*, vol. 33, no. 6, pp. 1025–1039, June 2015.
- [18] O. Simeone, A. Maeder, M. Peng, O. Sahin, and W. Yu, "Cloud radio access network: Virtualizing wireless access for dense heterogeneous systems," *Journal on Communications and Networks*, vol. 18, no. 2, pp. 135–149, April 2016.
- [19] *IEEE 802.11 standard*, <http://www.ieee802.org/11/>.
- [20] R. M. Karp, *Reducibility Among Combinatorial Problems*. New York: Plenum, 1972.
- [21] J. Yang, S. C. Draper, and R. D. Nowak, "Learning the interference graph of a wireless network," *CoRR*, vol. abs/1208.0562, 2012. [Online]. Available: <http://arxiv.org/abs/1208.0562>
- [22] M. Kalisch and P. Bühlmann, "Estimating high-dimensional directed acyclic graphs with the PC-algorithm," *Journal of Machine Learning Research*, vol. 8, pp. 613–636, May 2007.
- [23] A. Tsybakov, *Introduction to nonparametric estimation*. Springer, 2008.